Performance Assessment of a Building-Integrated Photovoltaic Thermal System in a Mediterranean Climate—An Experimental Analysis Approach

Karol Bot [1,*] , Laura Aelenei [1] , Hélder Gonçalves [1] , Maria da Glória Gomes [2] and Carlos Santos Silva [3]

[1] Laboratório Nacional de Energia e Geologia (LNEG), 1649-038 Lisbon, Portugal; laura.aelenei@lneg.pt (L.A.); helder.goncalves@lneg.pt (H.G.)
[2] CERIS, Department of Civil Engineering, Architecture and Georesources (DECivil), Instituto Superior Técnico, Universidade de Lisboa, 1049-001 Lisbon, Portugal; maria.gloria.gomes@tecnico.ulisboa.pt
[3] IN+, Center for Innovation, Technology and Policy Research /LARSyS, Department of Mechanical Engineering (DEM), Instituto Superior Técnico, Universidade de Lisboa, 1049-001 Lisbon, Portugal; carlos.santos.silva@tecnico.ulisboa.pt
* Correspondence: karolbot@live.com

Abstract: The experimental investigation of building-integrated photovoltaic thermal (BIPVT) solar systems is essential to characterise the operation of these elements under real conditions of use according to the climate and building type they pertain. BIPVT systems can increase and ensure energy performance and readiness without jeopardising the occupant comfort if correctly operated. The present work presents a case study's experimental analysis composed of a BIPVT system for heat recovery located in a controlled test room. This work contribution focuses on the presentation of the obtained measured value results that correspond to the BIPVT main boundary conditions (weather and room characteristics) and the thermal behaviour and performance of the BIPVT system, located in the Solar XXI Building, a nZEB exposed to the mild Mediterranean climate conditions of Portugal.

1. Introduction

1.1. Background and Motivation

The use of solar energy systems integrated into buildings is an urgent need, considering the impacts of the building sector on energy use and the usual non-renewable sources of energy [1]. The increase of building energy demands and shrinking resources has significantly impacted the standard of living for future generations. The development of solutions and alternative energy sources in the built environment has gained attention and became a priority in the last years. When facing climatic changes, buildings have to be prepared to respond to both heating and cooling challenging demands, and an example of a case study in this context may be found in [2]. Indeed, the design of energy-efficient and affordable integrated solutions in buildings represents a very ambitious target.

The European Building Standards are trying to respond to these challenges, namely since 2010 with the publication of the European Commission. Directive 2010/31/EU of the European Parliament and of the Council of 19 May 2010 on the energy performance of buildings [3], where new levels of performance—nearly zero energy performance—are required for new and existing buildings. This Directive had been the subject of several updates to date.

According to [4], the nearly zero-energy building (nZEB) does address the adoption of energy efficiency measures and the application in an integrative manner of renewable energy systems to supply the building energy consumption. Photovoltaic systems integrated in the envelope of the building have become a vital concept for new and existing buildings to fulfil the nZEB performance demands; however, their integration still constitutes a

defying step in building design, from either architectural and installation, operation and use perspectives. A deeper look into the contribution of solar systems to the nZEB design concept, specifically for Portugal, may be found in [5]. In this article, the authors studied four renovation scenarios in which solar energy was applied to achieve the nZEB concept. In [6], a feasibility study for the implementation of solar powered nZEB residences for the southern Europe is developed, and the authors shown that with a moderate cost increase, the implementation of nZEBs are possible for this specific region.

The photovoltaic modules coupled with a building envelope through a ventilated air cavity can improve the indoor thermal conditions and reduce building energy demand by using the heat resulting from the conversion of the solar energy incident to PV. On the other hand, the heated air inside the cavity between the PV module and building envelope can cause overheating problems when this cavity is closed as elevated operating temperatures can reduce the conversion efficiency of photovoltaic solar energy modules.

These scenarios can be overcome by ventilating the air cavity formed between the PV module and the building envelope, and also the heat released in the conversion process from PV being can be successfully recovered for indoor heating (hence the Building Integrated Photovoltaic Thermal—BIPVT—name given to the system). Details of the concept and further explanation of BIPVT system design and operation may be found in [7].

The BIPVT systems can offer a quick response to the demand, supporting a high adaptivity level [8]. BIPVT systems have intrinsic dynamic behaviour, that depends on the climatic conditions. This very dynamic behaviour shall not be an obstacle to their implementation on a building's façade. Indeed, it shall be considered that these elements may complement the performance of typical building constructive elements that have an intrinsic slower response to weather variations [9]. If correctly designed and operated, the BIPVT may provide, by these means, more flexibility to a building's energy system operation.

1.2. Objectives and Structure

This work aims to develop a detailed experimental investigation of a BIPVT system to assess its performance and thermal behaviour. The experimental part of the investigation complements the authors' numerical work given in [10]. The main novelty of this work is the study of this systems in a Mediterranean climate—characterized by mild temperatures—, as BIPVTs are often used in a quite different type of climate, in which there is a more accentuated temperature gradient between outdoors and indoors during the year and especially in colder temperatures. The other innovation is the fact that the system, located on the vertical façade in this case study, was built as new and as a whole façade (not a prototype or an add-on), and during the operation stage an improved behaviour for a building located in a Mediterranean climate was shown in comparison with a usual façade element, providing good comfort and supplying energy at the same time. The SolarXXI building, a net zero energy building (NZEB) living lab and the BIPVT integrated façade are thoroughly monitored, contributing to a better understanding of the system and insights on how to improve it in future buildings.

This experimental analysis' insights allow understanding the PV integration design in a new office building and the corresponding real behaviour during one year of operation, during a typical winter and summer month, and provide a detailed analysis related to a typical winter climatic condition day. The experimental study is a valuable approach to understanding these systems' real behaviour under Mediterranean climatic conditions and can be used for numerical analysis and model validation.

The experimental data have also been used to analyse the system thermal/electrical efficiency and key performance indicators used as inputs to the performance evaluation equations, increasing the reliability of the results in regard to support to decision making of installation of these systems in similar buildings in the future.

The research presented by this work also aims to contribute to the sustainable development of the building's sector by presenting the experimental analysis results of a BIPVT

system installed in the Solar XXI living laboratory facilities in Lisbon (Portugal, Mediterranean mild climate). It focuses on the obtained measured values that correspond to the system's real conditions of operation of the variable/component under study, given the BIPVT boundary conditions existent at the moment (weather data and room temperature). This study also contributes to the sense that the BIPVT system is located in an nZEB, a high-performance building already having sustainable constructive solutions that reduce the energy demand.

The presented work reports experimental results of one of the several solar integrated system solutions designed, developed and tested in the framework of NZEB_LAB Research Infrastructure on Solar Energy Systems, located in Lisbon, Portugal [11]. This research infrastructure integrates experimental capacities and equipment in the area of the solar energy system (Solar Energy Laboratory), in the area of materials (Laboratory of Material and Coatings) and the SolarXXI building—a Nearly Zero Energy Building (nZEB) office. More details of the NZEB_LAB Research Infrastructure may be found in [12].

This paper's structure is as follows: a first section with the introduction in the context and motivation of the research of these kinds of systems, followed by a brief of the literature review of the BIPVT in Section 2. The case study, together with the experimental setup, is presented and described in Section 3. The experimental results and corresponding analysis of the thermal behaviour are given in Section 4. Finally, the conclusions are presented in Section 5.

2. Building Integrated Photovoltaic Thermal System—Summary of Related Works

In comparison with solar thermal collectors and photovoltaic systems, integrated systems employ both technologies in the same system, generating both thermal energy and electricity. Many classifications can be adopted in order to better characterize these kinds of systems due to their complexity and multi-use functions. For example, a very simple classification is presented by [13], where the authors synthetically present a classification based on the integration, operation mode, application and type of approach for BIPVT systems. In this work and according to with integration type, the PV can be considered as a stand-alone element (PVT), as an integrated structural element in building façade and roof (BIPV), as technical devices added to the building (BAPV) and sometimes as an "add-on" component when a PV panel can be used as an external component, for example as a shading device. When the BIPV can also produce thermal energy for water or air heating, as previously mentioned, it can be considered a BIPVT.

A brief summary of some studies is presented in Table 1, including some examples of these kinds of systems according to system type, integration solution, the approach adopted, application objective and study objective.

In [14], an extensive review on PV/T systems is presented, being of particular interest to works concerning the design of innovative energy façade elements due to the novelty of the systems presented. The study reviews the structure guidelines and working instruments of the PV/T façade systems, execution, control procedures and building applications. They highlight the use of electrochromic coatings as the most used smart coating for thermal applications in PV systems and also highlight that concerning PV shading, the external shading is the most utilized due to its low initial costs. The authors also state that algae growth façades and folding façades (complex geometry) shading systems are as yet rising solutions, with high initial investment costs and requiring professional installers. They are, indeed, a promising arrangement because of their multi-purpose capabilities. Dynamic shading systems were found to reduce structure cooling power utilization by 12% to 50%. In [15], a survey of a significant number of shading systems on the main façades facing south or north (depending on the hemisphere, referred to as Sun-oriented façades) is presented, considering studies that have been published after 2010, segmenting the study into opaque and translucid elements.

In a most recent study of [16], the state of the art Sun-oriented control systems for façades are introduced, with a comparative assessment of Sun-powered control systems

and with guidelines for the improvement of new ones. It incorporates multifunctional frameworks and modelling with BIPV and thermal energy generation. Complementarily, in [9], the authors survey BIPV and BIPVT advancements, and an energy and exergy examination of BIPV and BIPVT systems is likewise discussed. This work reviews the ongoing innovation advancements around the world. In [17], the state of the art of double-skin BIPV façades is developed with a focus on their thermal analysis. In [18], an in-depth review is provided considering the concept, classification and assessment of emerging active building-integrated solar thermal/PV technologies.

In [19], the authors proposed a modular adaptive solar façade, in order to couple the element with the very dynamic environment surrounding the building boundaries. The energy behaviour and aesthetic expression of the façade can be managed to provide high spatio-temporal resolution responses. The design process and operational plan are described, along with simulation results of the thermal behaviour and power production/consumption. In [20], the authors elaborated on the energy performance of a ventilated photovoltaic façade under varied ventilation modes and controlling modes for different climacteric conditions, aiming to improve the energy conversion efficiency.

In [21], a prototype of a BIPVT was constructed based on thermal and electrical energy, aiming to achieve visual comfort and shading control through the system application. In this article, the prototype was evaluated under various conditions to characterize its performance. In [22], a study on energy evaluation of a photovoltaic wall with the use of either natural convection incited or fan-helped ventilation system was presented. A vertical photovoltaic Sun-oriented wall was introduced on the façade of a pre-assembled outside test room. The prototype development was manufactured with two economically accessible photovoltaic modules, an air cavity and an insulated back layer.

In [23], the authors propose a modular hybrid photovoltaic/solar thermal façade technology that uses integrated collector and storage solar technology. In light of a patented solar thermal diode concept and shaped into a flat modular profile incorporating PV cells/module, the proposed system aims to heat the indoor environment, provide hot water and also generate electricity. In [24], the authors proposed an arrangement of a building-integrated photovoltaic, thermoelectric wall solution. It is examined using a numerical model comprising of a PV framework and thermoelectric brilliant wall element. The thermal and electrical components of the system under cooling prevailing atmospheres was numerically researched utilizing an iterative system model. The presentation of the system is optimized by a near investigation with a traditional solid wall.

In [25], the study investigates the outcomes of a solar transparent photovoltaic window, focusing on angles of incidence, thermal gains using direct solar gains and energy generation. In [26], the proposed BIPVT system prototype is composed of air collectors connected to an air handling unit to manage the airflow. The solution works based on two applications, namely heating and cooling needs.

In [27], a BIPVT system is analysed. There is a focus on the improvement of the articulation between electrical and thermal efficiencies and heat transfer through the structure. These articulations between thermal and electrical efficiencies are substantially crucial for various climatic conditions and diverse façade BI-SES designs. The system modules have been intensely studied for their energy, exergy and operational attributes with and without associated air pipe. In [28], a BIPVT system has been analysed for residential applications, assessing active and passive operational applications. In [29], they built up an incorporated model for evaluating the techno-financial execution of the BIPVT on façades, with an emphasis on energy demand and supply.

The authors of [29,30] presents a novel solution where a BIPVT is combined with a phase change material as a solution for thermal energy storage combined with air cavity ventilation. The results are presented in terms of numerical analysis and experimental one and also an economic analysis where the solution is compared with other BIPV solutions and traditional building components. In [31], a solution of a combined BIPV with water storage is presented experimentally for thermal performance assessment of the system.

Table 1. Summary of related works.

Reference	System Type	Integration	Approach	Application	Study Objective
[14]	BIPV and Wind Turbine System	Façade-shading (add on)	Simulation-CFD	Hybrid combined with wind turbine	Solar energy potential
[16]	Ventilated BIPV curtain walls	-	Simulation-CFD Experimental	-	Sensitive analysis, thermal performance
[19]	The Adaptive Solar Façade	Add-on, shading	Architectural concept	Shading	Architectural integration
[20]	Semi-transparent photovoltaic façade	Ventilated façade	Experimental-prototype	Ventilation, cooling	Thermal and ventilation performance
[21]	BIPV solar air collector	Prototype	Simulation-CFD Experimental-prototype	Hybrid, Mechanical ventilation	Thermal and power performance
[22]	Photovoltaic solar wall	Prototype	Simulation-dynamic experimental-prototype	Hybrid, Mechanical ventilation	Energy performance
[22]	Hybrid photovoltaic/solar thermal	Prototype	Experimental- prototype	Hybrid, storage, no ventilation	Performance characterisation
[24]	Solar photovoltaic, thermoelectric radiant wall	-	Simulation	Solar cooling	Energy-saving potential
[25]	Window integrated CdTe	-	Simulation-design	Ventilated cooling	Building energy savings
[26]	BIPV—air handling unit	Prototype, façade, ad-on	Experimental-lab. Prototype simulation	Hybrid, Ventilated mechanically	Optimal tilt angle
[27]	Building Integrated Opaque Photovoltaic (BIOPVT)	Design, roof	Simulation	Ventilated air cavity and without air cavity	Characterization, performance
[28]	BIPVT	Design, roof, façade	Simulation -TRNSYS	Hybrid, heat exchanger	Solar contribution, Economic performance
[29]	Distributed solar generation system	-	Simulation—Finite element	-	Estimation of the building energy demand and supply
[30]	BIPVT-phase change materials	Façade, design, prototype	Simulation Matlab-Simulink	Ventilation, heating and cooling, storage	Thermal performance
[13]	BIPVT-Phase Change Materials	Façade, prototype	Experimental, prototype, testing facility	Ventilation, heating and cooling, storage	Techno-economical performance
[31]	BIPV-Water Storage	Façade	Experimental	CFD	Thermal and storage performance

The BIPVT proposed in this study goes somehow beyond state of the art and the representative studies presented in Table 1. The proposed BIPVT system was integrated since the early stages of a designed building project as a building structure element. Since the construction stage, the monitoring system was integrated, permitting continuous monitoring, comparing with most of the experimental studies, which refer to laboratory prototypes tested in laboratory conditions and not in a real environment. Moreover, the BIPVT proposed is designed to work in any kind of climatic condition as a cooling or heating passive solution, compared with the majority of the BIPV solution that is specifically designed for heating or cooling. It worth also mentioning the importance of integration of this solution in the façade of an office building located in the mild Mediterranean climate towards the assessment of its NZEB performance.

3. Experimental Investigation

3.1. Case Study Description

The case study section describes the details of the location and weather, building characteristics, BIPVT system characteristics and operation modes. This work's case study object was detailed described in a previous work published by the authors and may be found in [10]. The case study considered represents the BIPVT façade of the Solar XXI nZEB living laboratory from the National Laboratory for Energy and Geology (LNEG, Lisbon, Portugal). It is known that the city of Lisbon has a subtropical Mediterranean climate and is classified as Csa (Köppen climate classification) [32–34], with the Atlantic Ocean wind influencing the rainfall but maintaining moderate temperatures.

Details and pictures of the test room may be found in [10], a previous work published by the authors. In summary, the test room has a south-oriented façade with a wall area of 3.97 m^2, in which the BIPVT is installed, and a fenestration surface (window with 2.82 m^2) that was closed during the whole experimental period. The room floor area is 16.70 m^2, and the room has one occupant with a typical service building occupation pattern during work hours. It is important to mention that this article, reporting the experimental part of the analysis, complements the numerical assessment that was developed in [10]. The numerical part in [10] used the results obtained by the experimental analysis to validate the computational models, providing reliability to the results. In [10], it is possible to find the parametric analysis containing different scenarios for system design and operation. In contrast to what was previously published in the numerical part of the Solar XXI's BIPVT analysis, the thermal efficiency was only possible to be obtained by means of experimental analysis, once the numerical analysis through dynamic simulation in EnergyPlus only provided average temperatures for the thermal zones, and for the calculation of thermal efficiency, it is necessary to have temperature data from different heights within the same thermal zone. The BIPVT systems consist of a total of 76 photovoltaic multi-crystalline silicon modules in the whole building and have an area of about 96 m^2 and 12 kW peak power installed. The PV modules have a power output of 160 Wp each, with a nominal efficiency of 12% and a power temperature coefficient (βc) of 0.005. In this context, the BIPV is an integrated element of the Solar XXI building since the design project. This case is not a renovation solution.

The added value of this solution in the first place the integration of solar energy systems-PV on the building footprint-façade. The base solution of the opaque façade is a brick wall externally insulated, a common solution used for new buildings in Portugal and fulfilling the reference construction characteristics.

As previously mentioned, these kinds of BIPVT systems are designed to improve indoor comfort using the heat recovered through the ventilation by opening interior vents during the sunny period in wintertime and by opening the exterior vents in the summertime to avoid overheating. These operation modes can be observed in Figure 1.
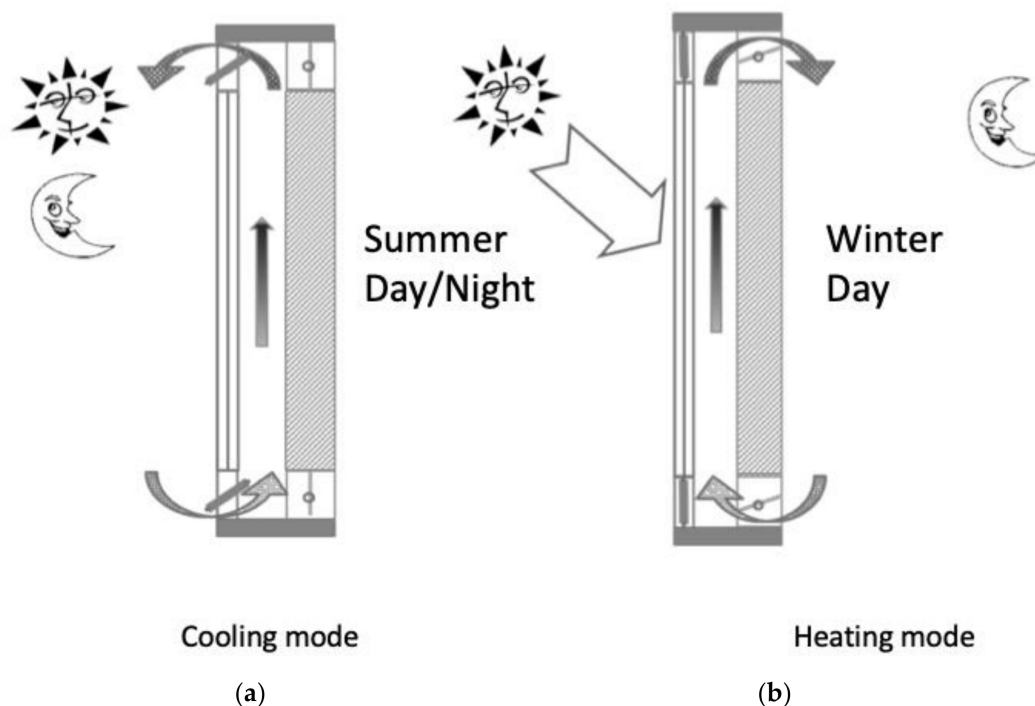
Figure 1. Manual operation work of a BIPVT system: (**a**) cooling mode; and (**b**) heating mode [35].

This BIPVT aims to increase the outlet temperature (T_{out}) compared to the inlet temperature (T_{inl}) of the system, having as source air the air volume from the adjacent thermal zone (room) when the aim is to heat indoors. They are composed of four PV modules with a total area per BIPVT system of 5.25 m^2, with four vent opening areas (inlet at the bottom and outlet at the top of the system, a set of two for the exterior (cool the modules during the summer), and a set of two for the interior (heat the room during the winter)) of 0.186 m^2 each. Between the interior wall and the PV modules, there is an air cavity of 0.16 m of thickness.

Concerning the properties of the air considered to be flowing or stationary in the air cavity, information that is used for the calculation of the convective heat flux is considered to have a density of 1.213 kg/m^3, the specific heat of 1006.7 J/kg.K, the thermal conductivity of 0.02544 W/(m.K) and viscosity of 1.79×10^{-5} kg/m.s [36]. The BIPVT is composed of the following constructive solutions and respective thicknesses, from the exterior to the interior: PV panel (0.003 m), air cavity (0.16 m), and the wall separating the adjacent thermal zone (test room) from the air cavity. The wall is composed of traditional plaster (0.03 m), EPS (0.06 m), brick masonry (0.22 m) and traditional plaster (0.02 m). The detailed thermal characteristics may be found in [10].

Figure 2, adapted from [10], shows the details of the geometry (Figure 2a) outdoor view of the system and (Figure 2b) system geometry. Temperature and heat flux sensors register the BIPVT thermal behaviour. There is a total of three temperature sensors located at the bottom (inlet), at the middle of the air cavity and the top (outlet). The temperature sensor locations are signalled with blue circles, whereas the heat flux sensors are marked with a red square. The temperature sensors located in the inlet and outlet openings are located 0.08 m in height from the bottom surface of the openings. The heat flux sensor used in this work's scope is the one located on the wall surface facing indoors (not the one located on the PV panel), and its height is 0.88 m above the inlet opening, at the same height as the air cavity temperature sensor. The dimensions of the air duct are also shown in the picture.
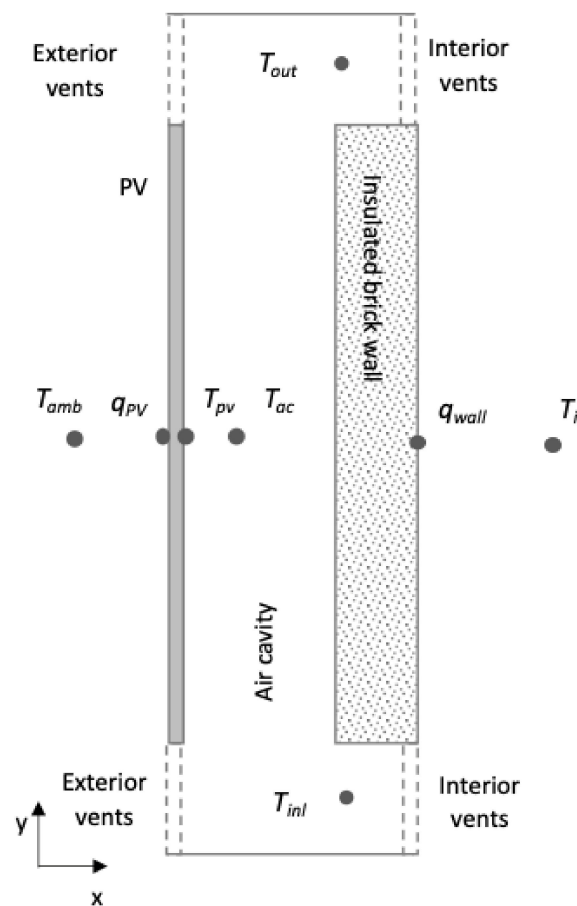
(**a**)   (**b**)

Figure 2. (**a**) Front view of the BIPVT systems in the Solar XXI building, (**b**) cross-section and dimensions.

3.2. Experimental Setup

The experimental approach allows the performance characterisation for the boundary conditions and element thermal behaviour registered during the experimental campaign. The observable variables of the BIPVT system are generically presented in Figure 3. The detailed description of sensors, in terms of observable variable, brand/model, range of measurements and accuracy are shown in Table 2.

Table 3 presents the month/year in which each segment of data was collected, at an average sampling rate of 37 recordings per hour.

Table 2. Details of the measurement instruments [10].

Observable Variable	Sensor Brand/Model	Range	Accuracy
T_i	Omega/PT100 [37]	−70 to 500 °C	0.03–0.07
T_{amb}	Omega/PT100 [37]	−70 to 500 °C	0.03–0.07
G_h	Kipp & Zonen CM6B 951765 [38]	200 to 4000 nm	<0.2%
G_D	Kipp & Zonen CHP1 100434 [38]	200 to 4000 nm	<0.2%
G_V	Kipp & Zonen CHP1 100434 [38]	200 to 4000 nm	<0.2%
G_d	Kipp & Zonen CM6B 983431 [38]	200 to 4000 nm	<0.2%
Air velocity	Testo 425 [39]	0 to 20 m/s	0.1
q_{wall}/q_{PV}	Hukseflux HFP01 [40]	−2000 to 2000 W/m^2	60×10^{-6} V/(W/m^2)
T_{ac}	Omega/PT100 [37]	−70 to 500 °C	0.03–0.07
T_{pv}	Omega/PT100 [37]	−70 to 500 °C	0.03–0.07

Table 3. Recording periods for each observed element.

Year					2018											2019		
Month	1	2	3	4	5	6	7	8	9	10	11	12	1	2	3	4	5	6
Weather data	✓	✓	✓	✓	✓	✓	✓	✓	✓	✓	✓	✓	✓	✓	✓	✓	✓	✓
Room temperature	✓	✓	✓	✓	✓	✓	✓	✓	✓	✓	✓	✓	✓	✓	✓	✓	✓	✓
BIPVT system	✓	✓	✓	✓	✓	✓	✓	✓	✓	✓	✓	✓	✓					

Figure 3. Experimentally measured variables of the system.

4. Results and Discussion

Employing experimental analysis, it is possible to observe and register real parameters and characteristics of the weather, BIPVT system, and test room in the study that will evaluate the façade components' performance. In [41], there is an extensive review for the energy assessment through experimental analysis—in which it is highlighted that the accuracy and long-time period of data are essential to bringing reliability to the study.

The experimental analysis is segmented into two main parts: (i) weather-related—outdoors ambient temperature (T_{amb}), direct normal solar radiation (G_D), diffuse horizontal solar radiation (G_d) and global horizontal solar radiation (G_h) and test room temperature (T_i)—the main boundary conditions of the system; (ii) BIPVT variables—PV module temperature (T_{pv}); outlet/inlet temperature gradient (ΔT); air cavity temperature (T_{ac}); conductive heat flux of the wall (q_{wall}). The experimental analysis results are used in the third part of the work to calculate the system's performance and set the relationship between variables. The performance is calculated based on the thermal efficiency (η_t) of the BIPVT system, as well as the dimensionless analysis.

Table 4 presents the temporal scale in which the experimental campaign and analysis were developed.

4.1. Weather Data and Room Temperature

The weather data was collected from the LNEG weather station to capture the most accurate values to represent the boundary conditions of the BIPVT system. The output of this phase was also used both for the control algorithms and for developing the weather files used in computational modelling of an associated study developed in [10].

During the year 2018, nearly 8328 valid hours of data were registered, with 432 missing hours due to recording failures or equipment maintenance. The major recording failures

concerning weather data of 2018 occurred in March and April (failure of the data logger), May (equipment failure), July and August (external calibration of the equipment), and December (power loss).

Table 4. Temporal scale of the analysis.

Parameters/Temporal Scale	Year	Season	Day
BIPVT variables			
PV module temperature	X	X	-
Air cavity temperature	X	X	-
Heat flux	-	-	X
Analysis			
Temperature gradient	X	X	-
PV module temperature/Air cavity temperature	X	X	-
Thermal efficiency	-	-	X
Dimensionless temperature	-	-	X

Figure 4 presents: (a) the ambient temperature and (b) ambient temperature in terms of frequency of occurrence. The annual temperatures are most concentrated between 10 °C and 21 °C but still accounts for many hours above 21 °C, whereas fewer hours a below 10 °C. The T_{amb} also hits extreme peaks of near 45 °C. Between June/2018 and October/2018, the temperature values were within this interval for a considerable number of hours. The annual temperatures hit a peak in August (44.03 °C), and its lowest in February (2.95 °C). The average yearly temperature was 16.43 °C.

The values for the annual solar radiation profile are provided in Appendix A. Figure A1 presents the values of global horizontal radiation. The G_h hit the highest values between July and August. Figure A2 presents the direct normal solar radiation values, and Figure A3 presents the values of the diffuse horizontal solar radiation. However, due to system maintenance, there is a lack of registers on some days of these months. In January and February, the highest value is near 600 W/m^2. The BIPVT system has better production of heat/electricity when the G_D is incident directly on the south-oriented façade. During the winter, the solar angle propitiates this production once the sun is lower in the sky than in the summer.

Overall, the year 2018 was a year with high-temperature peaks during a few days of the summer period. Low temperatures (below a considered T_{comf}) have a significant occurrence, showing that there are plenty of hours during the year in which BIPVT elements would be useful for heating the space while reducing energy consumption through the use of other equipment for the same purpose.

The indoor temperature (T_i) was also recorded. For the year 2018 and the first days of 2019, the T_i is fully presented to have a picture of whole year temperature fluctuations, as in Figure 5, and specific periods of winter and summer are presented in Appendix B, in Figures A4a and A4b, respectively. Due to the passive solutions integrated into the design of the Solar XXI building, that as explained, is already a net-zero energy building, it is possible to see that the most of annual hours are within the comfort zone, having the most critical periods in January/2018 and February/2018 due to energy needs for heating, and in August/2018 and September/2018 due to energy needs for cooling. The registered T_i are mostly within T_{comf} and it is possible to see that the lower temperatures, as expected, happen at night when the room is not receiving solar gains and is losing heat to the exterior.
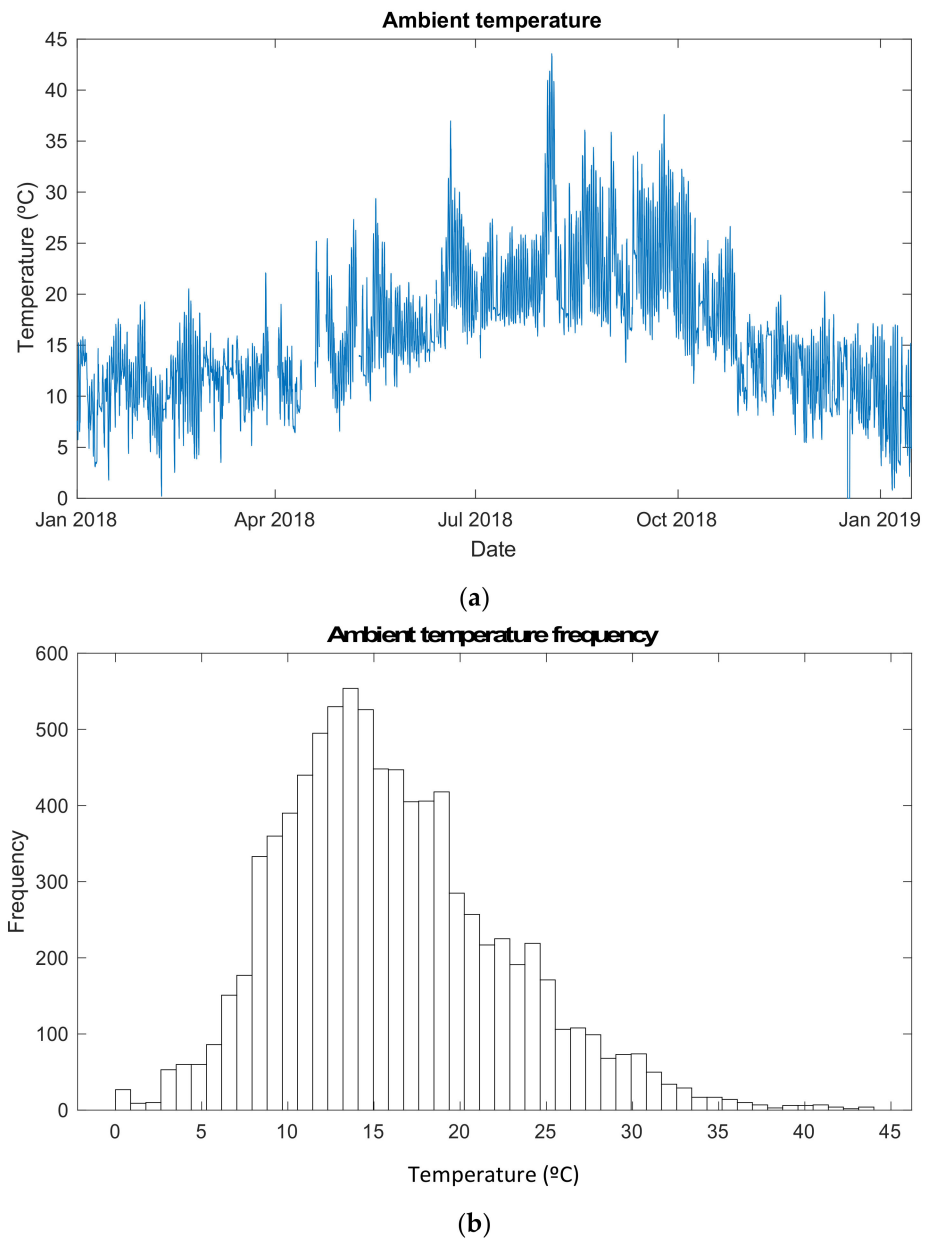
(**a**)

(**b**)

Figure 4. (**a**) Ambient temperature; (**b**) ambient temperature frequency.

4.2. BIPVT System Yearly/Seasonal Behaviour

4.2.1. Photovoltaic Module Temperature

A PV module exposed to solar radiation has its temperature usually above the ambient temperature, being dependent on the solar radiation intensity, ambient temperature, wind velocity, and the technology and structure used to compose this module. In this thesis's scope, factors as wind velocity and the impact of technology, material, and structure are not analysed. Complementary analysis of the effects of different factors on the T_{pv} may be found in [42,43], where there is a framework presented in how the wind effect may be included in the PV module temperature and is significantly useful for studies in which the PV module temperature are derived from calculations. This sub-section aims to evaluate the T_{pv} purely by directly measuring the temperature in its interior surface T_{pv}, that is the surface directly in contact with the adjacent air cavity and use the obtained values for the further theoretical calculation of the PV module η_e.
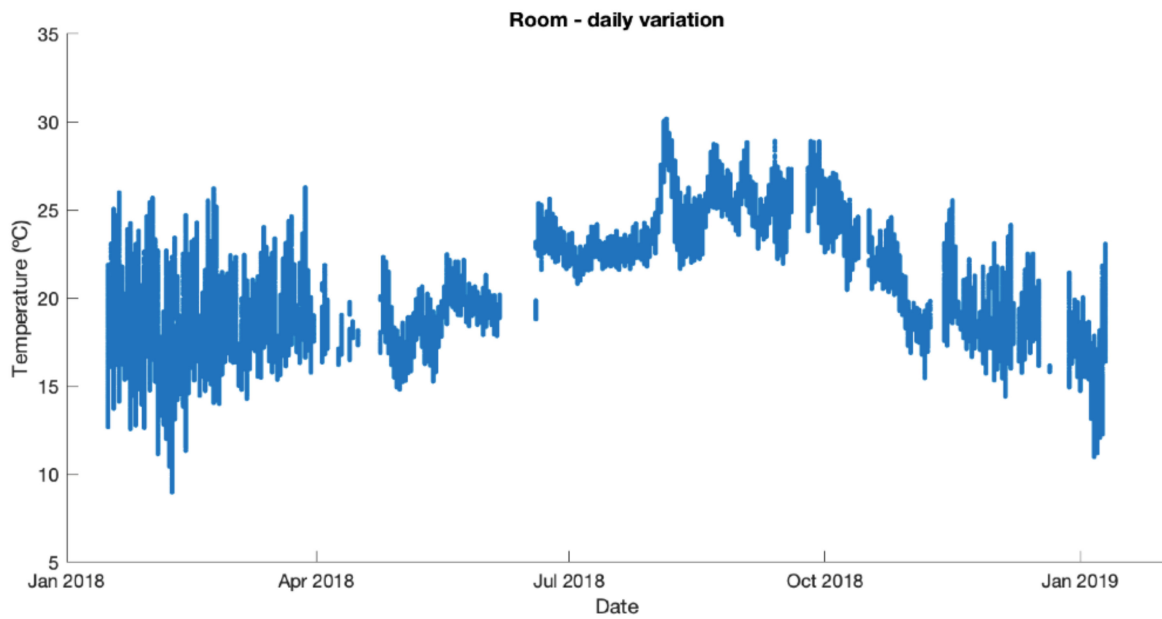
Figure 5. Yearly room temperature.

The yearly obtained values for the T_{pv} (Figure 6), and in detail, the temperature fluctuations in February and July are shown in Appendix B (Figure A5a,b), shows a considerable superficial temperature amplitude in the PV module, concerning its inner surface. Overall, during the year 2018, the maximum values can overcome 60 °C, while the minimums can be as low as 0 °C. It shows that the PV module, as is known, is a significant source of heat to interior air cavities when is exposed to direct solar radiation to generate heat to the room through convection and work as a heat recovery system. The high temperatures may, however, decrease the electrical efficiency of the photovoltaic generation—despite the present study focusing mainly on the potential of the systems to reduce the nominal energy needs for heating to achieve the comfort of the occupants of the adjacent thermal zone, for which the high temperatures of the PV module accomplish the purpose.
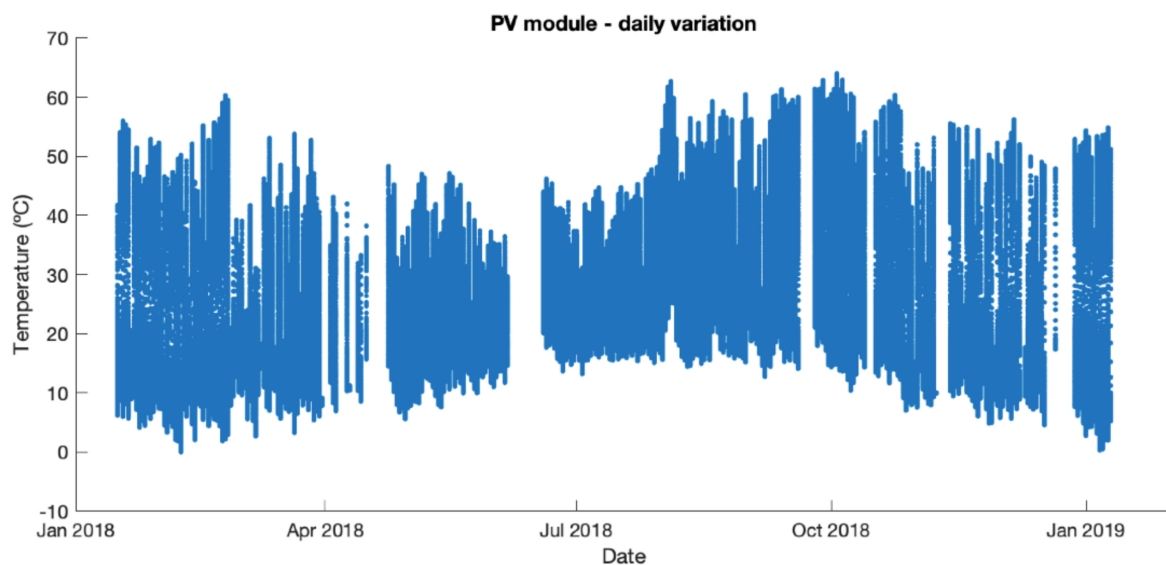
Figure 6. Yearly PV module temperature.

In a short amount of time as a day, the temperatures show variations from near 60 °C to near 5 °C, showing the effect of the direct solar radiation in heating the module. It is possible to note that the peaks in colder months are higher than the peaks in warmer months, despite warmer months present lower temperature amplitude during the day. It is due to the solar angle in relation to the south façade.

From the experimental values of T_{pv}, it is possible to conclude that the obtained values are higher than the T_{amb} during the Sun exposure hours, being this an excellent passive source of heat for the adjacent air cavity, in which the circulating air will heat the thermal zone. The variation on the T_{pv}, as in February, is very abrupt—having in about one-third of the daily hours a temperature over 30 °C. However, to serve as a heat source, it is enough that the panel hits a higher temperature than the air cavity temperature. The T_{pv} profile, in BIPVT systems, is adequate to the operation of the heat recovery system in usual working hours, as was the case of Solar XXI Building. On the other hand, during the warmer months, it is indicated to allow external air circulation, avoiding the air cavity's overheat and increasing the η_e of the system by reducing the T_{pv}, once the system will not be operating to heating the test room.

4.2.2. Air Cavity Temperature

As previously mentioned, the T_{pv} directly affects the T_{ac}, once it is the primary source of heat during the Sun exposure hours. It considers the T_{ac} for the BIPVT system as a point temperature obtained for the half-height of the air cavity, where only one sensor is available. However, it is essential to highlight that the temperature within the air cavity is not homogeneous—and to complement the study in terms of sensor availability limitations, as was shown in [10], in which it was demonstrated that the temperature gradient varies in both the horizontal and vertical directions. The T_{inl} and T_{out} within the air cavity, present a gradient value, which is shown in the next subsection. The T_{ac} is impacted not only by the T_{pv}, but also by the interior wall temperature (the boundary between the system and the thermal zone), by the possible openings or leakage surfaces that allow the air mixing between the air from outdoor and/or air from indoors, and by the thermal bridges existent in the system.

Given these considerations, the experimental results of the BIPVT air cavity temperature are shown in Figure 7, and details in Appendix B, Figure A6a,b. During the year 2018, the maximum T_{ac} (middle height of the system) are near 35 °C, while the minimum T_{ac} hits 1.47 °C. The amplitude of the temperatures is lower during June/2018 and July/2018, with an increased minimum temperature when compared to the winter months. In August/2018, the T_{ac} hits its maximum registered, with 56.57 °C. The annual average temperature of the air cavity is 19.13 °C.
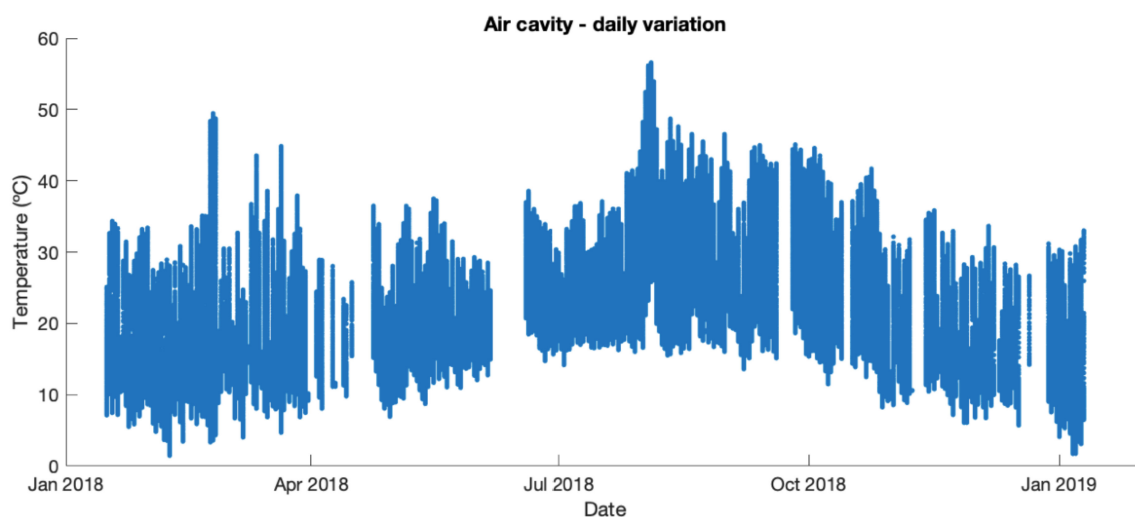

Figure 7. Yearly air cavity temperature.

There are considerable daily fluctuations on the BIPVT T_{ac}, due to the PV module's thermal resistance that separates this air cavity from the outdoors. It is possible to see that during the summer, the daily BIPVT T_{ac} amplitude is lower than in the winter, also reflecting in smaller ΔT (presented in the next sub-section), which is also influenced by the room temperature and would be later reflected in efficiency reduction, since the efficiency calculation formula is based on the temperature gradient for the convective heat flux. In February, during all the registered days, the T_{ac} was, for hours with higher Sun exposure, higher than the minimum established T_{comf} (20 °C), meaning that the system would be useful for heating the adjacent thermal zone and contributing to raising its temperature by the convection generated due to the ΔT within the air cavity. The obtained results for the T_{ac} are consistent with other BIPVT system prototypes previously evaluated the Solar XXI façade [44] from previous years. However, this work presents a significant improvement in terms of number of data samples acquired, being more representative in terms of periods of analysis.

4.2.3. Outlet/Inlet Temperature Gradient

As previously mentioned, being T_{pv} is the primary source of heat to the air cavity, within the air cavity, a ΔT is generated due to convection. This ΔT refers to the temperature difference between the T_{out} and the T_{inl} of the BIPVT system at a given moment and is responsible for the convective heat flux generated by the system when calculating its further η_t.

In Figure 8, the ΔT between the outlet and inlet registers ($T_{out} - T_{inl}$) of the temperature sensors is calculated and shown. During the winter months, the ΔT is more elevated due to the lower T_i in comparison to summer months, and to the higher values of G_D due to the solar angle in winter. These values could reach 14 °C in some peaks for the monitored period, although in general, they reached near 6 °C. Despite being a low-temperature gradient value, 6 °C is enough for the system to actuate as a heat recovery source if the thermal zone temperature is lower than the air cavity temperature.
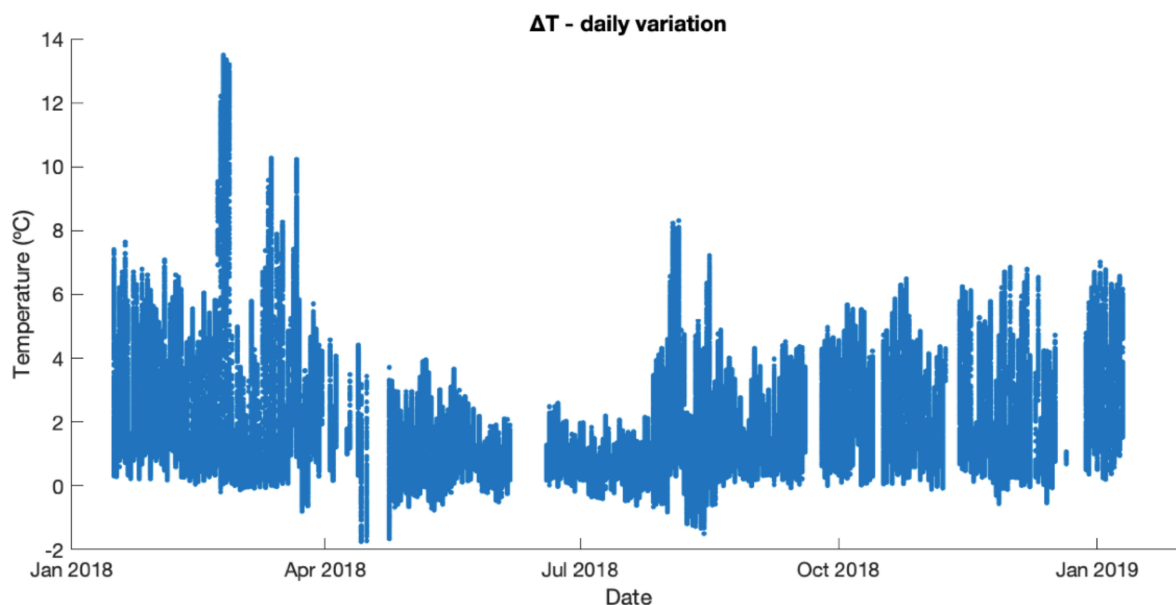

Figure 8. Yearly ΔT gradient.

In the summertime, the ΔT assume values as low as 1 °C, being possible to see even a few periods in which the T_{inl} are higher than the T_{out}. As is possible to see in the detail in Appendix B (Figure A7a,b), the amplitude is higher during February in an order varying from 4 °C to 13 °C. This factor will also be reflected in the thermal performance of the system under real-condition testing. As expected, during most of the year, the T_{out} is higher

than T_{inl}. The ΔT in a system impacts the airflow velocity once the heat source will generate a vertical upwards airflow within the air cavity due to buoyancy forces resulting from density differences due to temperature variations, as was possible to see in the associated study [10].

4.3. Thermal Behaviour—Yearly/Seasonal Analysis

The relationship between the BIPVT system measured variables is also essential, in particular between T_{ac} and T_{pv}. It is recognised that the T_{ac} is not dependent only on T_{pv}, having the T_{amb} and T_i also impact the temperature of the air cavity. However, the T_{pv} The solar radiation exposure and the PV module are the primary heat source of the system under operating hours. For this reason, this relationship is assessed here.

Figure 9 shows the results for the relationship between the annual T_{ac} and T_{pv} in a scatter plot, where it is possible to see that there is a positive correlation between these two variables. As the T_{pv} increases, the number of possible values for the T_{ac} do also increase, meaning that for a certain T_{pv}, a broader range of T_{ac} values exist. The lower the T_{pv}, the more concentrated are the possible values for the T_{ac}.
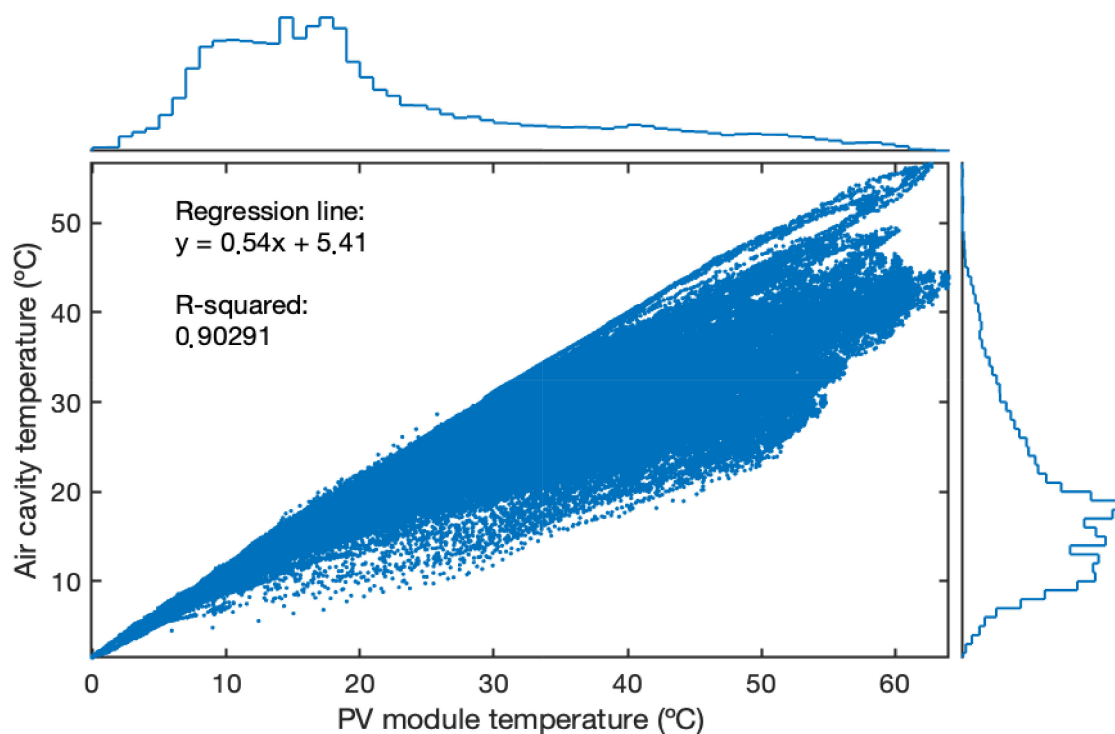
Figure 9. Relationship between air cavity and PV module temperature for the entire register period, with the histogram of the temperature bins of 1 °C each bin.

In some cases, the T_{ac} can be slightly higher than the T_{pv}, due to the thermal gains in the room, thermal inertia of the interior wall and possible position of the vents. The best-fit trendline representing this relationship is characterised as the approximation of this relationship (T_{pv} and T_{ac}) demonstrated by the equation graph.

The R^2 value refers to the goodness of fit and is a fraction between 0.0 and 1.0. The higher the R^2 value, the more accurate the prediction of the relationship may be considered. However, it is necessary to recognise that the R^2 has its limitations, once cannot be used to determine if there is any kind of bias in the acquired data under analysis. In the scope of this study, it only aims to provide preliminary insights into the relationship. It demonstrated that the relationship is broader during winter (with less confidence), while is more straightforward during the summer (with more confidence), increasing the predictability accuracy, as in Figure 10a,b. The night periods have considerable impact on

the results of the best-fit line, as during the night the temperature is very similar to the air cavity temperature, and as so may be considered a bias in the relationship results, once the hours in which the PV module is cold due to the lack of solar availability are almost half of the day.
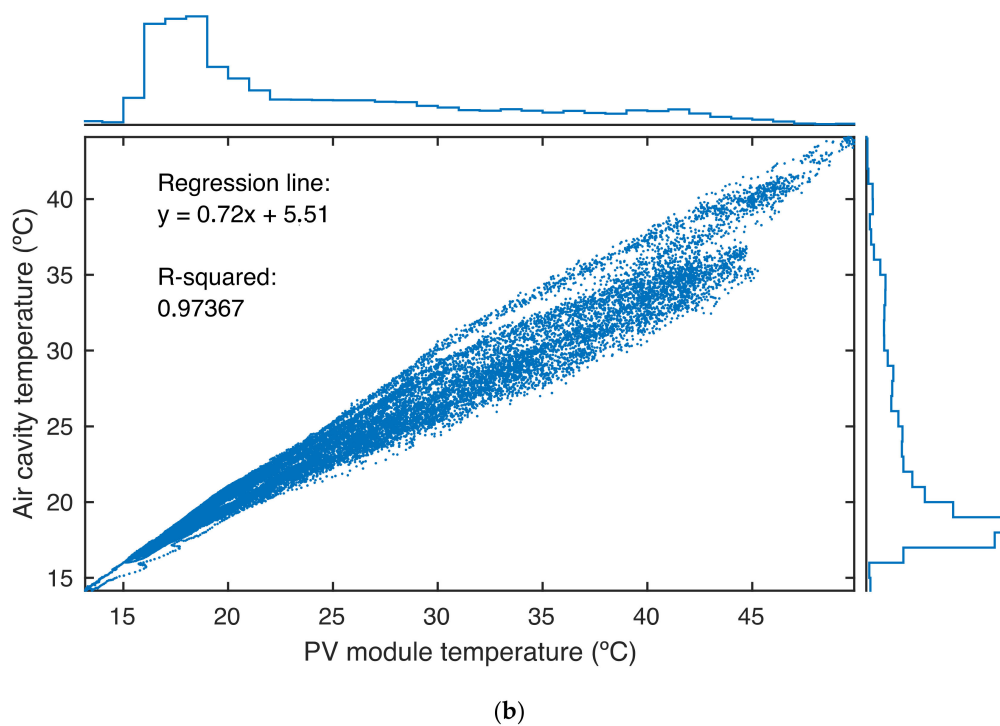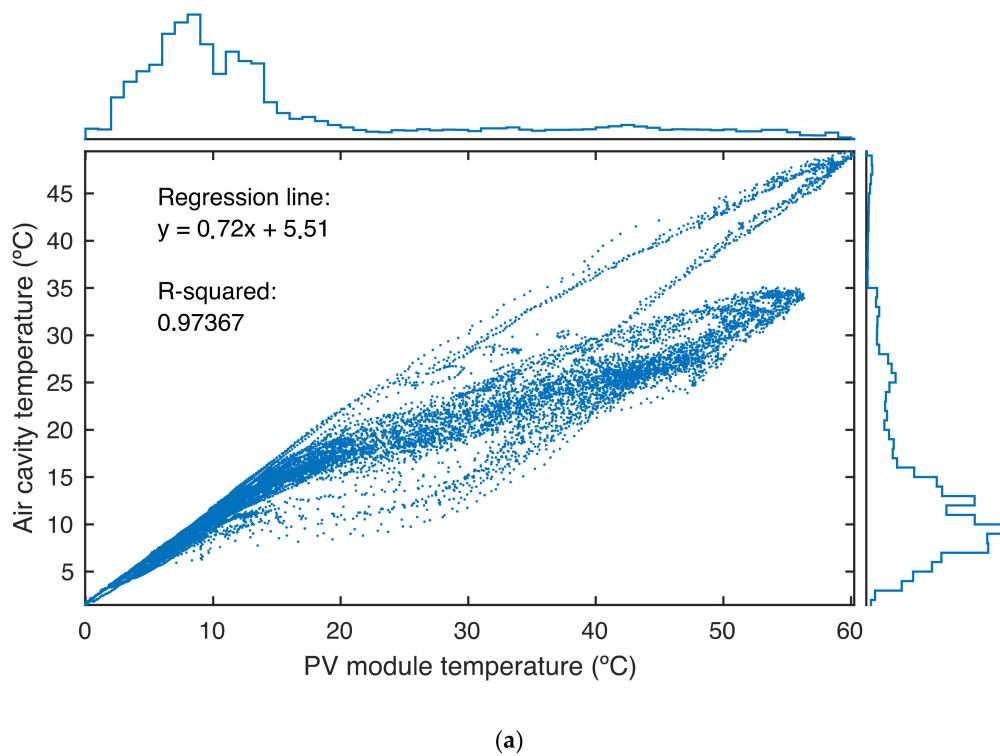

(**a**)

(**b**)

Figure 10. Relationship between air cavity and PV module temperature, with the histogram of the temperature bins of 1 °C each bin, for (**a**) February/2018; (**b**) July/2018.

Considering the different temperature sensors present inside the system (air cavity, PV module, inlet, outlet) and outdoors, there are outlier temperatures, higher than the statistical maximum of the year under the register. During the year, 50% of the T_{ac} is between 13 °C and 24 °C, while 50% of annual T_{pv} are between 14 °C and 28 °C. Annual temperatures of the outlet are slightly higher than the inlet, confirming that the existent q_v alongside the air cavity, reflecting the impact of ΔT on the η_t of the system.

As a conclusion for this relationship, there is a relationship between both temperatures, but it is also necessary to recognise that T_{ac} is not a single-valued function of T_{pv}, because the performance of the BIPVT system is affected by many other factors. The relationship between the variables could be improved by creating a broader set of variables (as adding ambient temperature as well), and also the co-relation analysis would be benefited to associate delay periods to each measured variable, as a couple of hours to days before the period in question, as is usual in forecasting models. The data acquired by this study may certainly be used to train forecasting models and increase the accuracy of the relationships, despite this not being the object of this work.

### *4.4. Thermal Behaviour—Daily Analysis*

This subsection also presents the details of a daily analysis, considering a winter day in which it is pertinent to the BIPVT system's operation and right sun-exposure weather conditions. The daily analysis of the registered values and calculations for the heat recovery BIPVT system is done considering 11 January 2019. The interior vents of the system were opened at 10:45 h and closed at 15:15 h. Figure 11a presents the registered values for the 24 h of the day, along with the direct normal solar radiation at the weather station (b). It is possible to see the effect of the vents' opening on the temperature of the air cavity, being responsible for a decrease of nearly 9 °C at the moments that followed 10:45 h (from 40 °C to 31 °C).

The PV module hit approximately 55 °C, slightly decreasing the temperature parabola with the opening of the vents. The system temperature achieved a difference of almost 20 °C from the T_{amb}, due to the solar gains on the PV modules, the thermal inertia of the interior wall and T_i. It is also possible to note the interior walls' excellent insulation when analysing the values from the heat flux sensor, which slightly vary from 5 W/m^2 to 48 W/m^2. On the other hand, the heat flux through the PV module achieved 210 W/m^2 at noon. During the vents opening hours, it is possible to see the detailed profile in Figure 11. For the period under investigation, the registered air velocity in the inlet was 0.01m/s (manually measured with an anemometer sensor, punctually during few minutes in the operation hours). It is essential to highlight that the air velocity in the inlet, for the BIPVT system, was not measured constantly due to the lack of a permanent sensor, and intrinsically vary during the day and the year due to many factors impacting on the air movement. It was assumed as presented in [10].

Due to the thermal inertia, it is possible to see that the system still slightly increases the temperature even with the decrease of the incident solar radiation. The T_{out} is lower than the T_{ac} in the order of 2 °C, due to the air mixing in the outlet, between the system air at a given temperature and the room air at another given temperature. Also, a difference of almost 10 °C was registered between the T_{out} and T_{inl}. The energy performance and efficiencies will be discussed in another section. Besides the measured variables presented here and the impact of the vents opening on the system thermal behaviour, other variables that are not under control and monitoring may be impacting the system, such as the wind speed.
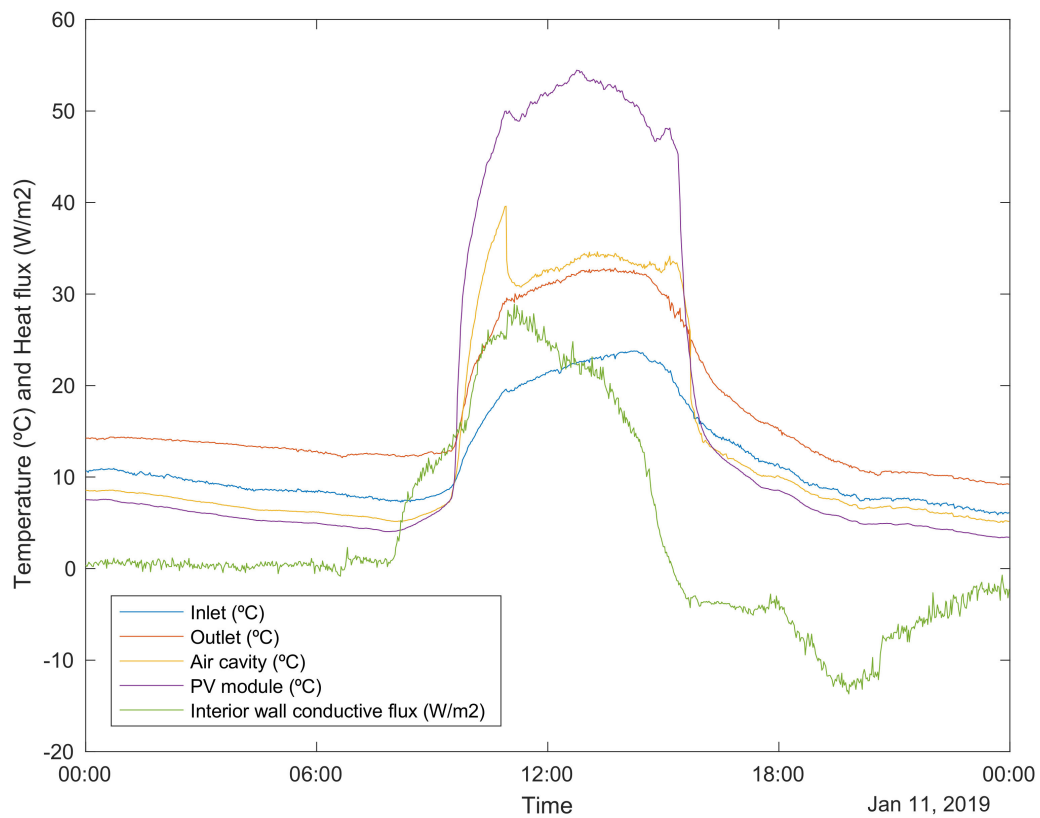
(**a**)
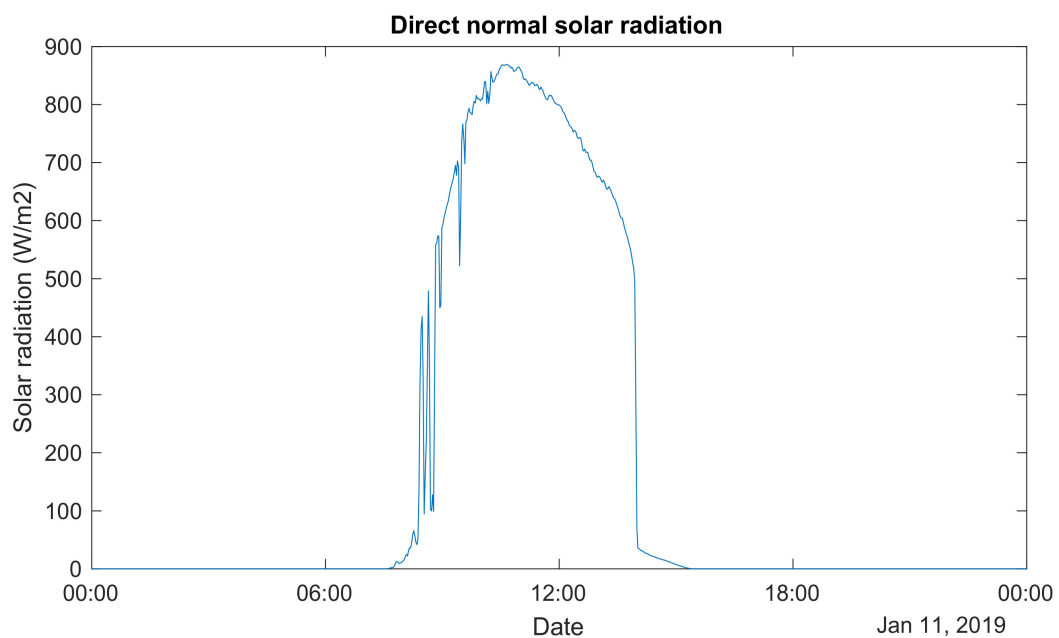
(**b**)

Figure 11. Daily behaviour: (**a**) the BIPVT system under manual operation, opened at 10:45 h and closed at 15:15 h, (**b**) direct normal solar radiation on the weather station.

4.5. Efficiency of the System

Generally, in most of the studies referred to in Section 2, the system's characterisation was made through the use of building performance indicators or construction performance

indicators, employing energy needs analysis to reach thermal comfort or by the study of the system efficiency. However, efficiencies and dimensionless analysis also characterise the system's heat transfer and performance, as presented by [45,46]. This study aims to determine the thermal efficiency of the system and also calculates the theoretical electrical efficiency in function of the module temperature.

The calculation of the thermal η_t (1) and the electrical η_e (2) efficiencies is presented below [47]. The thermal efficiency convective heat flux (q_v) (3) component is calculated based on the obtained results for the inlet (T_{ini}) and outlet (T_{out}) air cavity temperatures and the mass flow rate that depends on the air flow velocity through the air cavity [10]:

$$\eta_t = \frac{q_{wall} + q_v}{G_V \times A} \tag{1}$$

$$\eta_e = \frac{P}{G_V \times A} \times \left(1 - \beta c \times \left(T_{pv} - T_{NOCT}\right)\right) \tag{2}$$

$$q_v = \dot{m} \times c_p \times \left(T_{out} - T_{inl}\right) \tag{3}$$

In an air-based thermal system, the q_v (3) plays an essential role in the η_t, once the aim of the system is heating the adjacent thermal zone based on the ΔT gradient generated within the air cavity. The calculation of the systems' energy thermal efficiencies took into consideration the q_v, that was calculated based on the results obtained by the experimental campaign, and the q_{wall}, directly obtained by the measurement campaigns.

The system's thermal efficiency for heating purposes was calculated and presented in Figure 12, considering the same opening hours. The slight increase in the efficiency is due to the decrease of the incident solar radiation in the vertical surface (G_V) (wall in which the BIPVT is installed), obtained by the second pyranometer, installed in this vertical surface. The η_t is nearly 4%. The uncertainty must be taken into consideration in regards to the calculation of the thermal efficiency. As in Table 2, the main uncertainties associated with thermal efficiencies calculated are the ones related to the sensor responsible for measuring the incident solar radiation in the vertical surface (possible error lower than 0.2%), and mostly the air cavity temperature sensor (possible error between 0.03 °C and 0.07 °C) and the air velocity sensor (possible error of 0.1 m/s), that directly affects the convective heat flux values. Considering the obtained value for 11:30 h, as presented in Figure 12, the related uncertainty could cause the value to vary in the order of nearly 0.5%.

The theoretical electrical efficiency of the modules is calculated by Equation (2) and also shown in Figure 12, taking into consideration a PV module normal operation condition temperature of 20 °C. It reaches 15.1% at 12:30 h. The theoretical power output (calculated based on the available area of PV modules, incident solar radiation, and theoretical efficiency determined in Figure 12) for the BIPVT system is also presented in Figure 12, and varies from 0.618 kW at 11:30 h, when the solar radiation assumes higher values, to 0.523 kW at 12:30 h, when the solar radiation is lower considering the presented period. The obtained solar power output is satisfactory given the building energy demand related to the nZEB concept.

The reduced thermal efficiency values may happen due to different causes. The BIPVT systems have a temperature gradient on the PV module itself, that although not being reported here given the fact that this study had only one surface temperature sensor (Figure 6) for the module, it is reported in [48]. This superficial temperature gradient in the modules is translated to the interior cavity, in the case of a BIPVT system, causing different conductive heat fluxes along the PV modules surface, with impacts on the air cavity temperature vertical profile. Also, when the vents are opened, there is a backflow on the outlet vent, in which point the thermal zone air mixes with the air cavity air at that height, contributing to reducing the outlet temperature in the operating hours of the BIPVT system with the purpose of thermal recovery—and this effect may be found in the computational fluid dynamics study developed by the authors in [10,49]. Considering that the thermal performance of the Solar XXI building is high, the thermal zones do not

reach considerable low values, as is possible to see in Figure 5, which implicates in a higher temperature of inlet, reducing the component of temperature gradient of the convective heat flux (3). Also, the $\dot{m}$ component of the equation is fairly low, as the system has natural ventilation. As was shown in the numerical part of the study published in [10], higher air changes from the room to the air cavity results in better performance, indicating that the use of forced ventilation could improve the thermal efficiency. In addition, Portugal is a country with mild temperatures during the year, which means that the temperatures are not very high or very low for an extended period during the year. The case study building is also considerably efficient in thermal aspects.
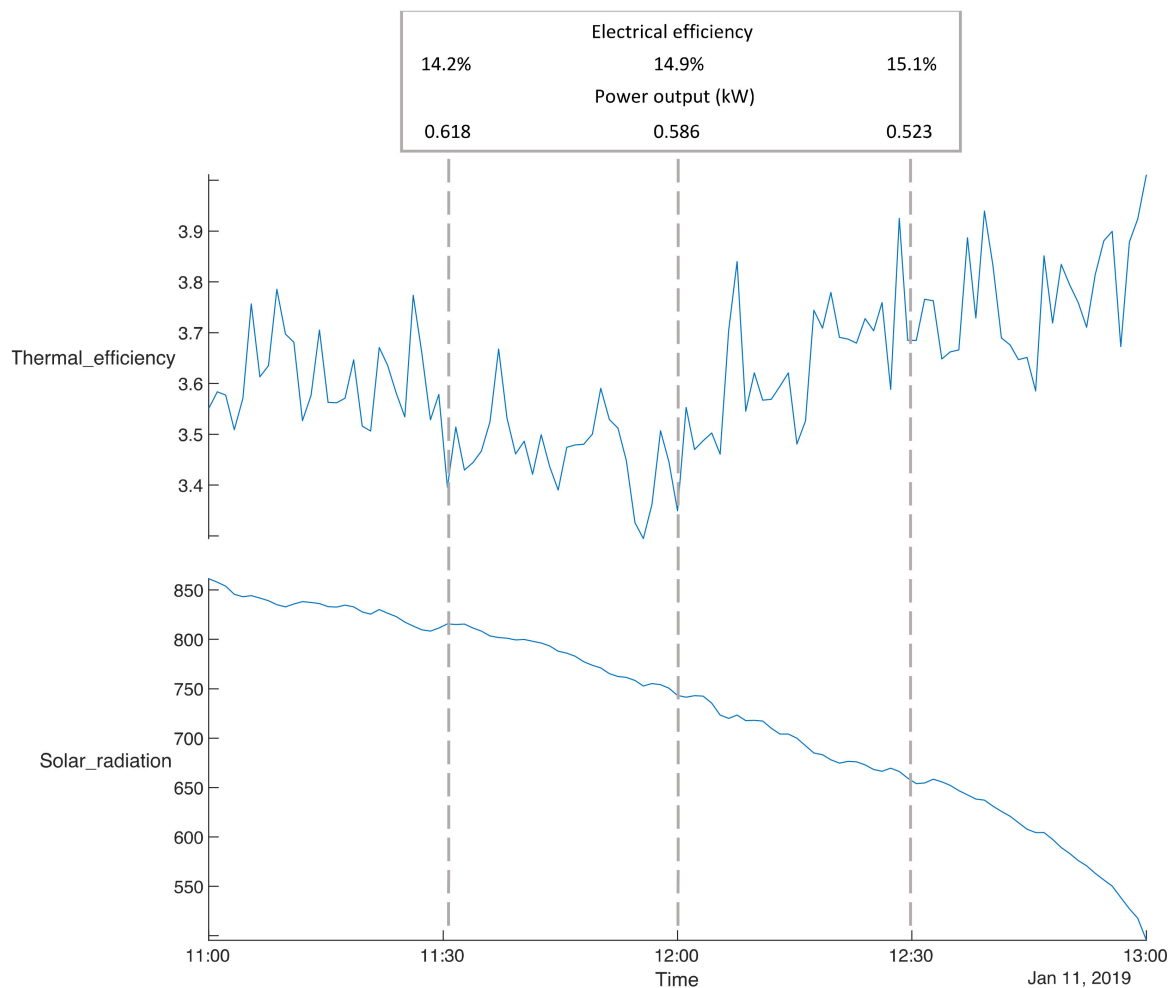
Figure 12. BIPVT system thermal efficiency (%) profile for heating purposes, electrical efficiency and direct solar radiation on the vertical surface (W/m^2).

Dimensionless thermal behaviour through a ventilated façade element may be based on the relationship between dimensionless height (*H**) (4) and dimensionless temperature (*θ exp*) (5), as is presented in Figure 13.

$$H^* = \frac{ys}{H} \qquad (4)$$

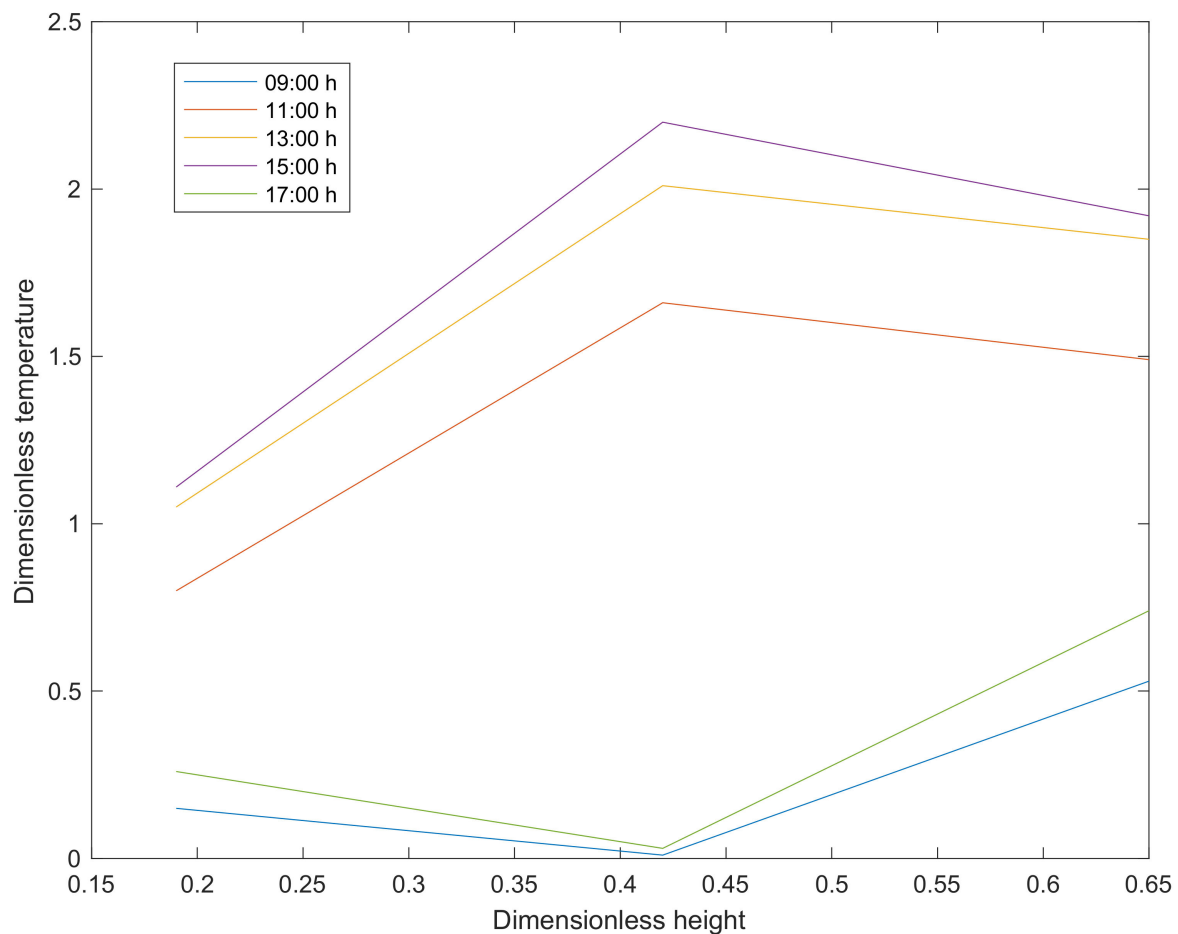$$\theta exp = \frac{Ty - Tamb}{Ti - Tamb} \qquad (5)$$

Figure 13. BIPVT dimensionless temperature and height (11 January 2019).

5. Conclusions

The building in which the case study is based is the Solar XXI building from the National Laboratory for Energy and Geology (LNEG, Lisbon, Portugal), which is recognised for having implemented a wide range of strategies to reduce the cooling and heating loads through solar control strategies and passive systems as buried pipes. The main building façade is composed of BIPVT systems that aim to generate electrical energy and act as a heat recovery system. These systems consist of 76 photovoltaic multi-crystalline silicon modules in the whole building and have an area of about 96 m^2 and 12 kW peak power installed.

In the present study, the experimental analysis was developed to obtain a detailed characterisation in real use conditions of a building integrated photovoltaic thermal system (BIPVT) installed in the façade of Solar XXI building from the National Laboratory for Energy and Geology (Lisbon, Portugal). The novelty of the work focus on the presentation of an extensive experimental campaign for the Portuguese climate, with the system being installed in a living lab facility in which many parameters are measured in a continuous basis. The publication of this results is important not only to serve as basis for the characterization of these systems in the mild Mediterranean climate, but also in the nZEB context. Three main aspects were studied: the weather parameters, the BIPVT parameters, and the room parameters.

The weather parameters were observed and registered during the whole year of 2018 and the first semester of 2019. The campaign was based on the register of ambient temperature, global horizontal radiation, diffuse horizontal radiation and normal direct radiation components. The indoor room temperatures also monitored during the whole period of analysis to calculate the efficiencies and determine the boundary conditions to be

used in the numerical analysis and model validation. It was concluded that the building already has an efficient thermal performance once the Solar XXI was projected to meet NZEB requirements. For so, the needs for cooling and heating are also reduced compared to the traditional constructive solutions being used in Portugal.

It presented the data concerning the T_{ac}, inlet and T_{out} in the air cavity, T_{pv}, and heat flux through the interior wall. The system presented a thermal efficiency of between 3.3% and 4% for heating purposes during the day studied in detail. However, it is necessary to highlight that these efficiencies are values that represent the behaviour of the system for the boundary conditions existent in the period considered for the calculation. In other words, the results may vary according to factors like solar radiation availability and T_i, and also indicates that forced ventilation may be considerably useful in similar situations to improve the efficiency results—remembering that in this study only natural ventilation was used. The theoretical calculated electrical efficiency obtained reached 15.1%. The calculation of efficiencies was purely based on these experimental campaign results. The system under study brings clear benefits to the buildings, mainly due to the electricity generated by the PV modules, and it was shown that it is also useful to contribute to heat the adjacent thermal zone in which it is installed.

The work was extensive in terms of the monitoring period and the number of variables analysed, and these data will serve in the future not only to validate computational models in terms of dynamic simulations, but also to train machine learning models and introduce the use of model-based predictive control to control the operation of the vents in a smart manner. Moreover, the presentation of such experimental campaigns may in the future contribute to the decision-making process in the point of view of architecture and engineering.

Author Contributions: Conceptualization, H.G. and L.A.; methodology, K.B. and L.A.; formal analysis, K.B. and L.A.; investigation, K.B. and L.A; data analysis, K.B., L.A., H.G., M.d.G.G. and C.S.S.; writing—original draft preparation, K.B. and L.A.; writing—review and editing, K.B., L.A., H.G., M.d.G.G., C.S.S.; supervision, L.A. and H.G.; project administration, L.A. and H.G.; funding acquisition, L.A. and H.G. All authors have read and agreed to the published version of the manuscript.

Institutional Review Board Statement: Not applicable.

Informed Consent Statement: Not applicable.

Data Availability Statement: Not applicable.

Conflicts of Interest: The authors declare no conflict of interest.

Nomenclature

H^*	Dimensionless height
ys	Sensor's height (m)
H	Total system height (m)
$\theta\,exp$	Dimensionless temperature
T_y	Sensor's temperature (°C)
T_{amb}	Ambient temperature (outdoors) (°C)
T_{pv}	PV interior module temperature (°C)
T_i	Indoor temperature (temperature of the room) (°C)

T_{comf}	Comfort temperature (20 °C to 25 °C)
T_{ac}	Temperature of the air cavity (°C)
ΔT	Temperature gradient (°C)
T_{inl}	Inlet temperature (°C)
T_{out}	Outlet temperature (°C)
G_h	Global horizontal solar radiation (W/m^2)
G_d	Diffuse horizontal solar radiation (W/m^2)
G_D	Direct normal solar radiation (W/m^2)
G_V	Incident irradiance on the vertical surface (W/m^2)
η_t	Thermal efficiency
βc	Power temperature coefficient
T_{NOCT}	Normal operation conditions temperature (°C)
η_e	Electrical efficiency
q_{pv}	Conductive heat flux of photovoltaic module (W/m^2)
q_{wall}	Conductive heat flux of wall component (W/m^2)
q_v	Convective heat flux (W/m^2)
A	Area (m^2)
c_p	Thermal capacity (kJ/(kg.°C))
$\dot{m}$	Air mass flow rate (kg/s)
$R.F.$	Register failures

Appendix A

Appendix A presents the supplementary material concerning the solar radiation data for the experimental period under consideration.
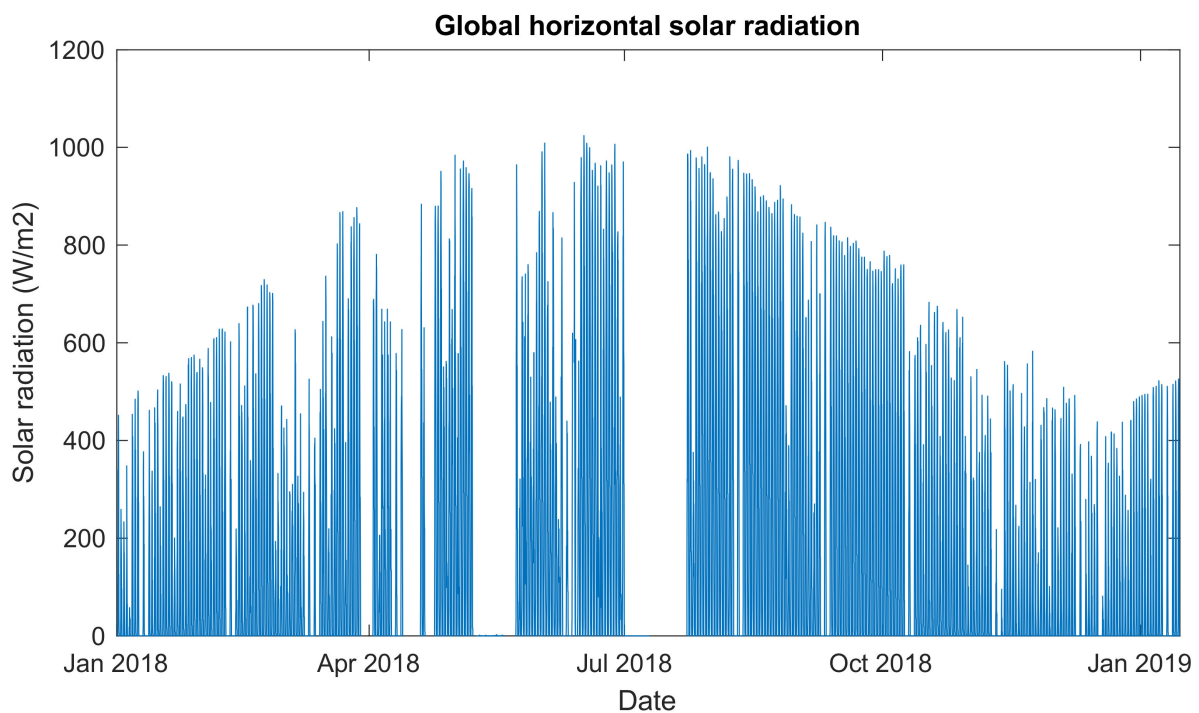

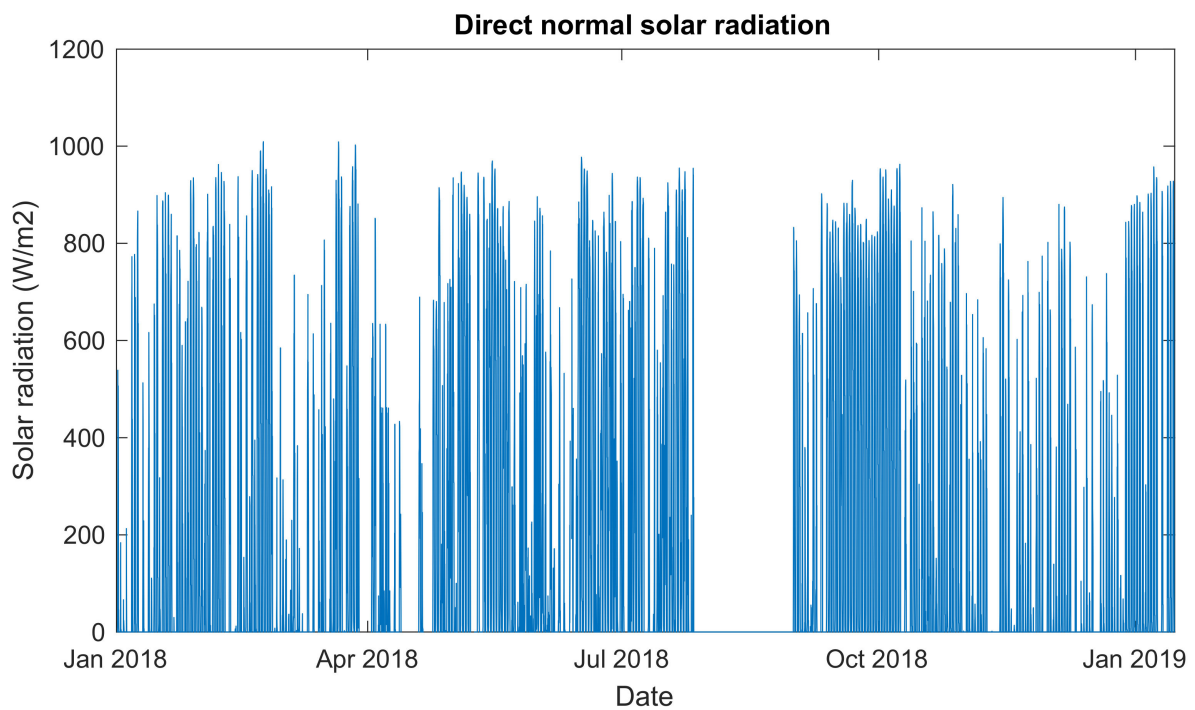**Figure A1.** Global horizontal solar radiation.

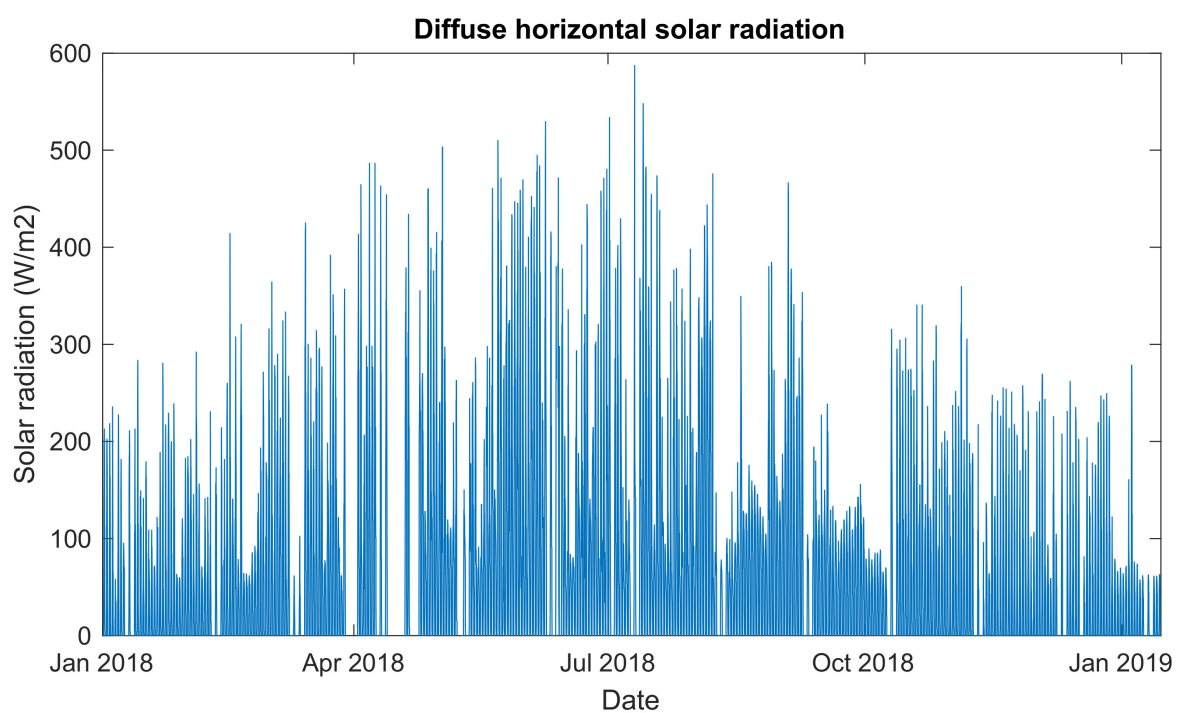**Figure A2.** Direct normal solar radiation.

Figure A3. Diffuse horizontal solar radiation.

Appendix B

Appendix B presents the supplementary results in terms of daily temperature variations for the months of February and July.
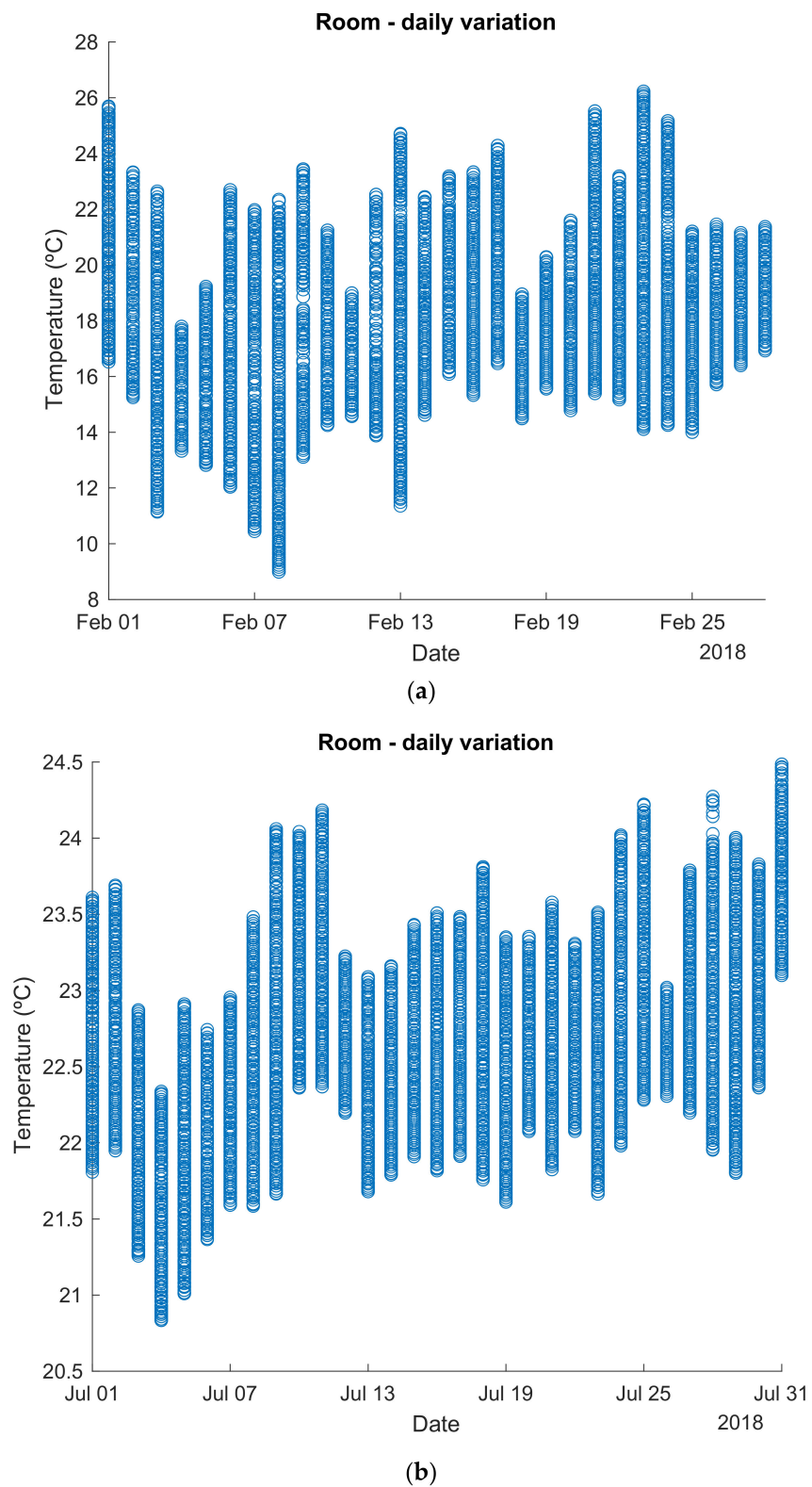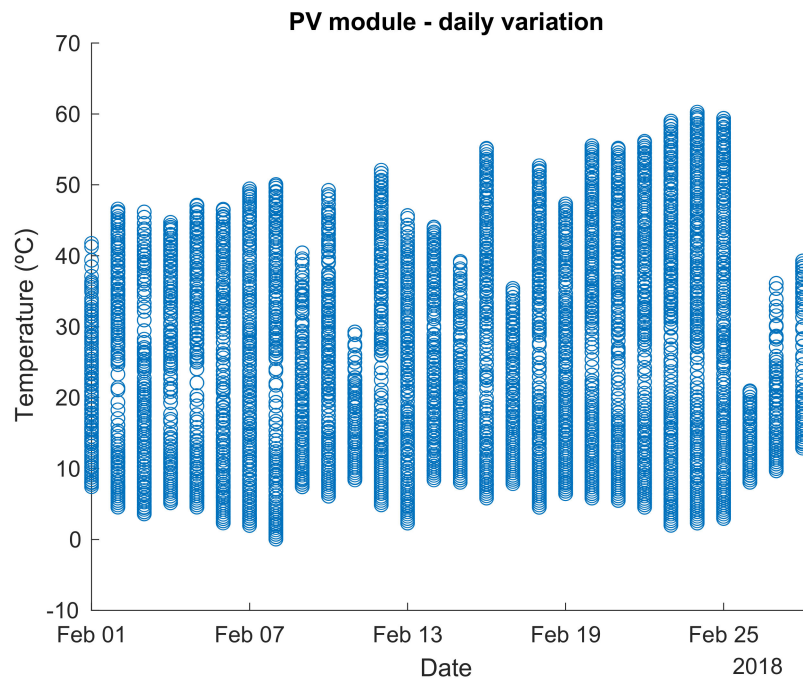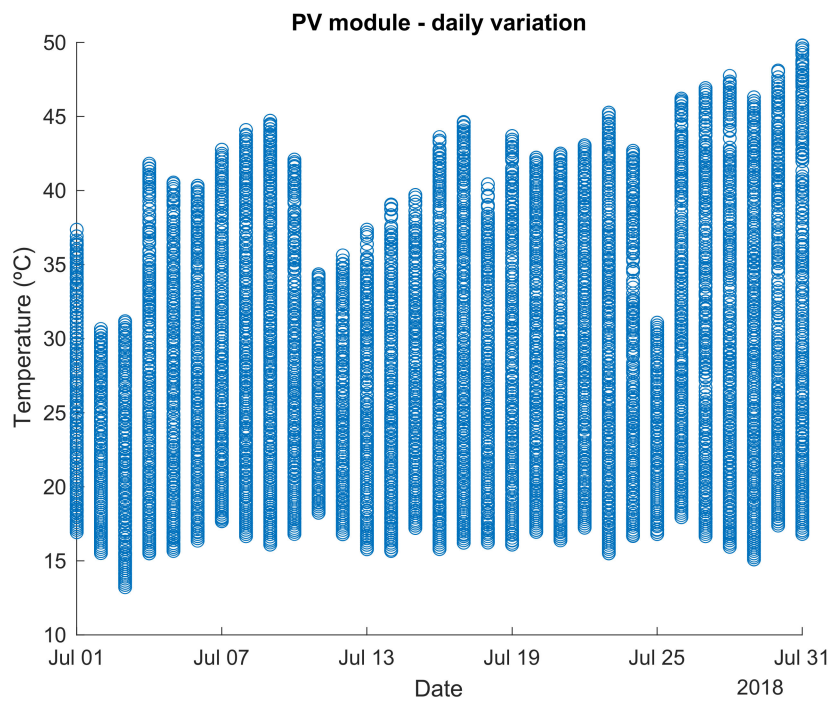
(**a**)

(**b**)

Figure A4. Detailed room temperature daily variation: (**a**) February/2018; (**b**) July/2018.

(**a**)

(**b**)

Figure A5. Detailed PV module temperature daily variation: (**a**) February/2018; (**b**) July/2018.

(**a**)

(**b**)
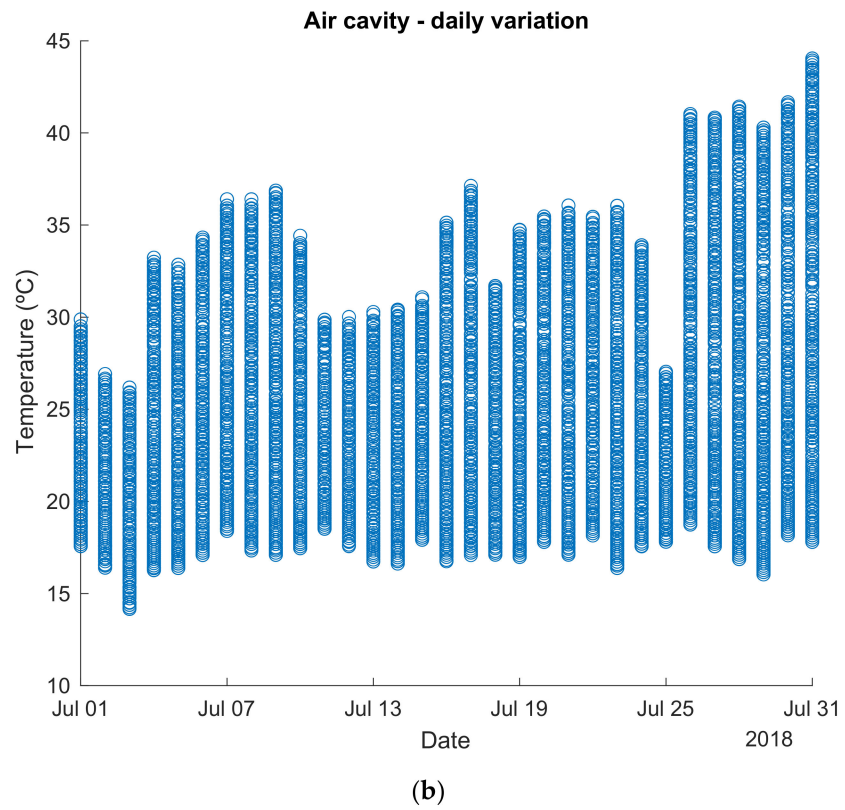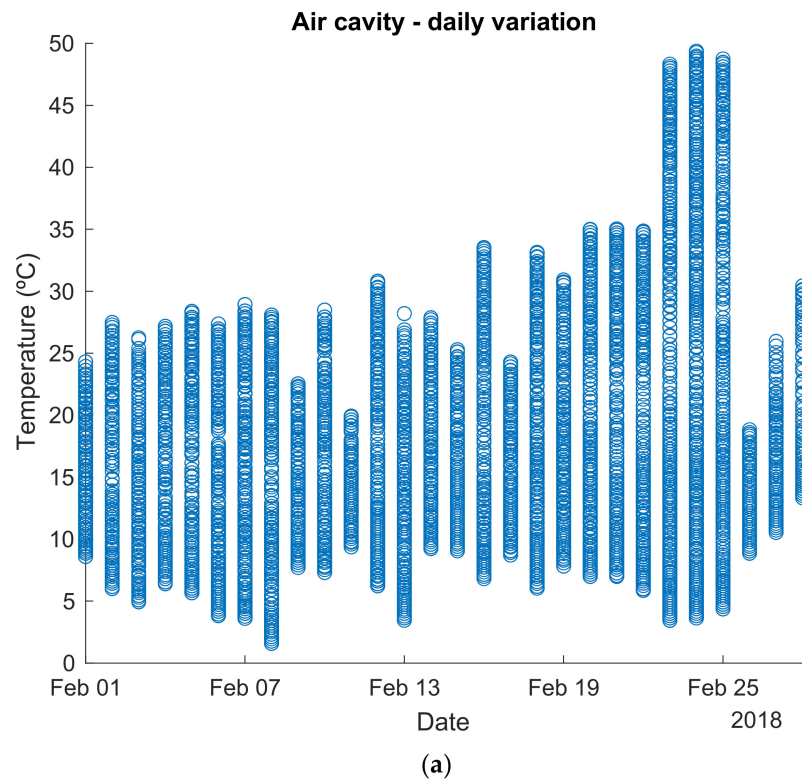
Figure A6. Detailed PV module temperature daily variation: (**a**) February/2018; (**b**) July/2018.
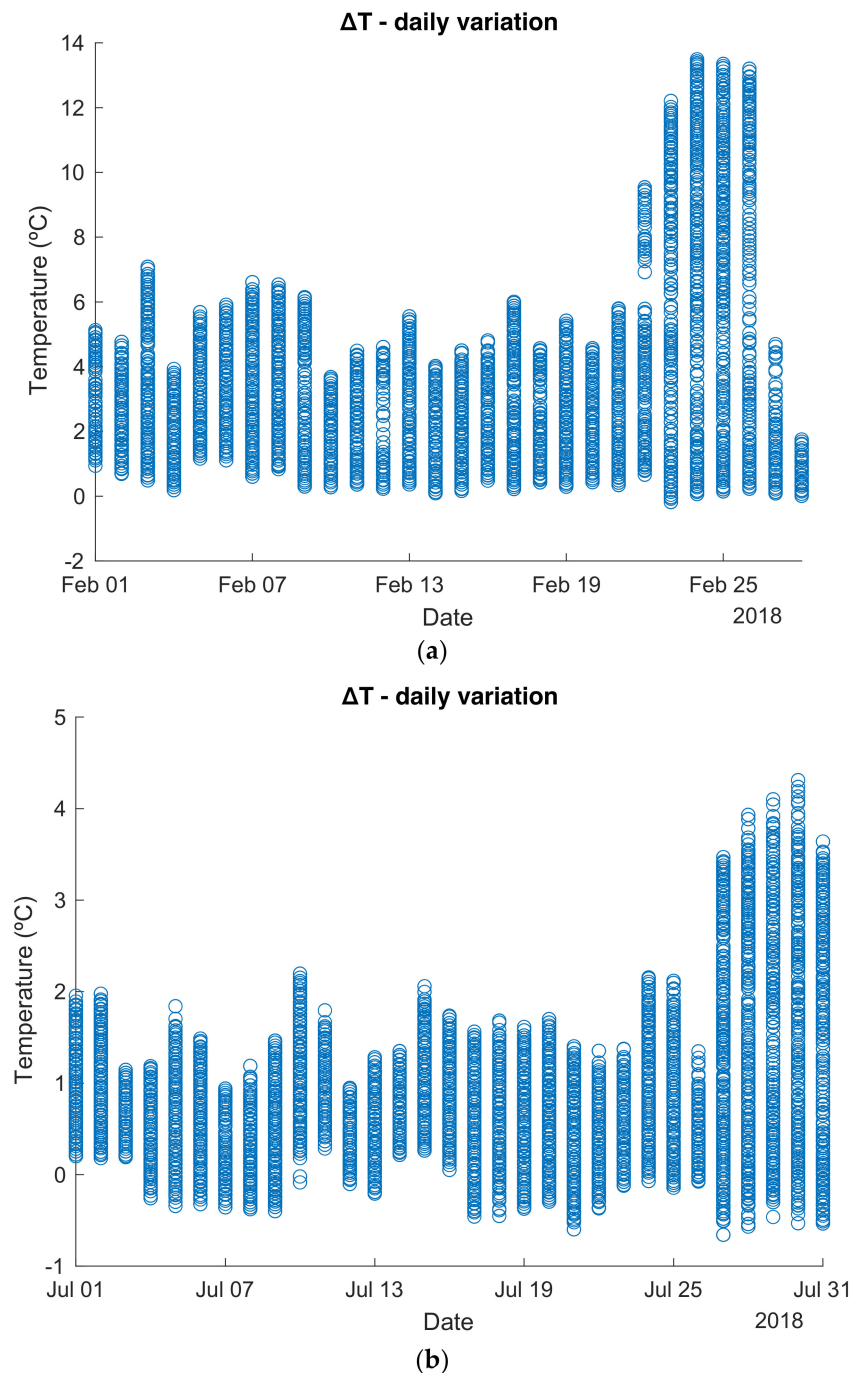
(**a**)

(**b**)

Figure A7. Detailed ΔT gradient daily variation: (**a**) February/2018; (**b**) July/2018.

References

1. Edelenbosch, O.Y.; Van Vuuren, D.P.; Blok, K.; Calvin, K.; Fujimori, S. Mitigating energy demand sector emissions: The integrated modelling perspective. *Appl. Energy* **2020**, *261*, 114347. [CrossRef]
2. Summa, S.; Tarabelli, L.; Ulpiani, G.; Di Perna, C. Impact of Climate Change on the Energy and Comfort Performance of nZEB: A Case Study in Italy. *Climate* **2020**, *8*, 125. [CrossRef]
3. European Parliament. Directive 2010/31/EU of the European Parliament and of the Council of 19 May 2010 on the energy performance of buildings (recast). *Off. J. Eur. Union* **2010**, *153*, 13–35.
4. Aelenei, L.; Pereira, R.; Gonçalves, H.; Athienitis, A. Thermal performance of a hybrid BIPV-PCM: Modeling, design and experimental investigation. *Energy Procedia* **2014**, *48*, 474–483. [CrossRef]

5. Silva, S.M.; Mateus, R.; Marques, L.; Ramos, M.; Almeida, M. Contribution of the solar systems to the nZEB and ZEB design concept in Portugal–Energy, economics and environmental life cycle analysis. *Sol. Energy Mater. Sol. Cells* **2016**, *156*, 59–74. [CrossRef]
6. Da Graça, G.C.; Augusto, A.; Lerer, M.M. Solar powered net zero energy houses for southern Europe: Feasibility study. *Sol. Energy* **2012**, *86*, 634–646. [CrossRef]
7. Agrawal, B.; Tiwari, G.N. *Building Integrated Photovoltaic Thermal Systems: For Sustainable Developments*; Royal Society of Chemistry: London, UK, 2010; ISBN 1849732000.
8. Burman, E.; Mumovic, D.; Kimpian, J. Towards measurement and verification of energy performance under the framework of the European directive for energy performance of buildings. *Energy* **2014**, *77*, 153–163. [CrossRef]
9. Debbarma, M.; Sudhakar, K.; Baredar, P. Thermal modeling, exergy analysis, performance of BIPV and BIPVT: A review. *Renew. Sustain. Energy Rev.* **2017**, *73*, 1276–1288. [CrossRef]
10. Bot, K.; Aelenei, L.; da Gomes, M.G.; Santos Silva, C. Performance Assessment of a Building Integrated Photovoltaic Thermal System in Mediterranean Climate—A Numerical Simulation Approach. *Energies* **2020**, *13*, 2887. [CrossRef]
11. Laboratório Nacional de Energia e Geologia NZEB_LAB Project. Available online: https://nzeblab.lneg.pt/?page_id=528&lang=pt (accessed on 28 February 2021).
12. Aelenei, L.; Gonçalves, H.; Carvalho, M.J.; Facão, J.; Joyce, A.; Diamantino, T.C.; Rodrigues, C.; Salema, D.; Rodrigues, R. Infraestrutura Nacional de Investigação na área de Energia: NZEB_LAB-Integração dos Sistemas Solares em Edifícios. In Proceedings of the CIES2020-XVII Congresso Ibérico e XIII Congresso Ibero-Americano de Energia Solar, Lisboa, Portugal, 3–5 November 2020; LNEG—Laboratório Nacional de Energia e Geologia: Amadora, Portugal, 2020; pp. 1091–1098.
13. Aelenei, L.; Pereira, R.; Ferreira, A.; Gonçalves, H.; Joyce, A. Building Integrated Photovoltaic System with Integral Thermal Storage: A Case Study. *Energy Procedia* **2014**, *58*, 172–178. [CrossRef]
14. Lee, J.; Park, J.; Jung, H.-J.; Park, J. Renewable Energy Potential by the Application of a Building Integrated Photovoltaic and Wind Turbine System in Global Urban Areas. *Energies* **2017**, *10*, 2158. [CrossRef]
15. Lai, C.-M.; Hokoi, S. Solar façades: A review. *Build. Environ.* **2015**, *91*, 152–165. [CrossRef]
16. Lai, C.; Hokoi, S. Experimental and numerical studies on the thermal performance of ventilated BIPV curtain walls. *Indoor Built Environ.* **2017**, *26*, 1243–1256. [CrossRef]
17. Agathokleous, R.A.; Kalogirou, S.A. Double skin facades (DSF) and building integrated photovoltaics (BIPV): A review of configurations and heat transfer characteristics. *Renew. Energy* **2016**, *89*, 743–756. [CrossRef]
18. Zhang, X.; Shen, J.; Lu, Y.; He, W.; Xu, P.; Zhao, X.; Qiu, Z.; Zhu, Z.; Zhou, J.; Dong, X. Active Solar Thermal Facades (ASTFs): From concept, application to research questions. *Renew. Sustain. Energy Rev.* **2015**, *50*, 32–63. [CrossRef]
19. Nagy, Z.; Svetozarevic, B.; Jayathissa, P.; Begle, M.; Hofer, J.; Lydon, G.; Willmann, A.; Schlueter, A. The adaptive solar facade: From concept to prototypes. *Front. Archit. Res.* **2016**, *5*, 143–156. [CrossRef]
20. Peng, J.; Lu, L.; Yang, H.; Ma, T. Comparative study of the thermal and power performances of a semi-transparent photovoltaic facade under different ventilation modes. *Appl. Energy* **2015**, *138*, 572–583. [CrossRef]
21. Chialastri, A.; Isaacson, M. Performance and optimization of a BIPV/T solar air collector for building fenestration applications. *Energy Build.* **2017**, *150*, 200–210. [CrossRef]
22. Dehra, H. An investigation on energy performance assessment of a photovoltaic solar wall under buoyancy-induced and fan-assisted ventilation system. *Appl. Energy* **2017**, *191*, 55–74. [CrossRef]
23. Smyth, M.; Pugsley, A.; Hanna, G.; Zacharopoulos, A.; Mondol, J.; Besheer, A.; Savvides, A. Experimental performance characterisation of a Hybrid Photovoltaic/Solar Thermal Facade module compared to a flat Integrated Collector Storage Solar Water Heater module. *Renew. Energy* **2019**, *137*, 137–143. [CrossRef]
24. Luo, Y.; Zhang, L.; Liu, Z.; Wu, J.; Zhang, Y.; Wu, Z. Numerical evaluation on energy saving potential of a solar photovoltaic thermoelectric radiant wall system in cooling dominant climates. *Energy* **2018**, *142*, 384–399. [CrossRef]
25. Barman, S.; Chowdhury, A.; Mathur, S.; Mathur, J. Assessment of the efficiency of window integrated CdTe based semi-transparent photovoltaic module. *Sustain. Cities Soc.* **2018**, *37*, 250–262. [CrossRef]
26. Ahmed-Dahmane, M.; Malek, A.; Zitoun, T. Design and analysis of a BIPV/T system with two applications controlled by an air handling unit. *Energy Convers. Manag.* **2018**, *175*, 49–66. [CrossRef]
27. Gaur, A.; Tiwari, G.N. Analytical expressions for temperature dependent electrical efficiencies of thin film BIOPVT systems. *Appl. Energy* **2015**, *146*, 442–452. [CrossRef]
28. Buonomano, A.; Calise, F.; Palombo, A.; Vicidomini, M. BIPVT systems for residential applications: An energy and economic analysis for European climates. *Appl. Energy* **2016**, *184*, 1411–1431. [CrossRef]
29. Oh, J.; Koo, C.; Hong, T.; Cha, S.H. An integrated model for estimating the techno-economic performance of the distributed solar generation system on building façades: Focused on energy demand and supply. *Appl. Energy* **2018**, *228*, 1071–1090. [CrossRef]
30. Aelenei, L.; Pereira, R. Innovative solutions for net zero-energy building: BIPV-PCM system—Modeling, design and thermal performance. In Proceedings of the 2013 4th International Youth Conference on Energy (IYCE), Siófok, Hungary, 6–8 June 2013; pp. 1–6.
31. Sousa, M.A.C.; Aelenei, L.; Gonçalves, H. Comportamento térmico de um protótipo BIPV combinado com armazenamentode água: Análise experimental. In Proceedings of the CIES2020-XVII Congresso Ibérico e XIII Congresso Ibero-americano de Energia Solar, LNEG-Laboratório Nacional de Energia e Geologia, Lisbon, Portugal, 3–5 November 2020; pp. 1167–1174.

32. Peel, M.C.; Finlayson, B.L.; McMahon, T. Updated world map of the Köppen-Geiger climate classification. *Hydrol. Earth Syst. Sci.* **2007**, *11*, 1633–1644. [CrossRef]
33. Rubel, F.; Kottek, M. Observed and projected climate shifts 1901-2100 depicted by world maps of the Köppen-Geiger climate classification. *Meteorol. Z.* **2010**, *19*, 135–141. [CrossRef]
34. Moret Rodrigues, A.; Santos, M.; Gomes, M.G.; Duarte, R. Impact of natural ventilation on the thermal and energy performance of buildings in a Mediterranean climate. *Buildings* **2019**, *9*, 123. [CrossRef]
35. Aelenei, L.E. Sistemas Prefabricados Para Edifícios de Baixo Consumo: Design; Modulação; Prototipagem e Testes 2016. Available online: https://fct.pt/apoios/projectos/consulta/vglobal_projecto?idProjecto=117782&idElemConcurso=4254 (accessed on 15 January 2021).
36. Ansys. Available online: https://www.ansys.com/products/fluids/ansys-fluent (accessed on 15 May 2018).
37. Omega. PT 100 Omega. Available online: https://www.omega.co.uk/section/rtd-pt100-probes-elements.html (accessed on 21 May 2020).
38. Kipp & Zonen. Pyranometers Kipp & Zonen. Available online: https://www.kippzonen.com/ProductGroup/3/Pyranometers (accessed on 15 January 2021).
39. Testo. Termoanemometer Testo 425. Available online: https://www.testo.com/pt-PT/testo-425/p/0560-4251 (accessed on 21 May 2020).
40. Hukseflux Heat Flux Plate. Available online: https://www.hukseflux.com/products/heat-flux-sensors/heat-flux-meters/hfp01-heat-flux-sensor (accessed on 21 May 2020).
41. European Comission. Directive 2002/91/EC of the European Parliament and of the Council of 16 December 2002 on the energy performance of buildings. *Off. J. Eur. Communities* **2002**, *L 1*, 65–71.
42. Schwingshackl, C.; Petitta, M.; Wagner, J.E.; Belluardo, G.; Moser, D.; Castelli, M.; Zebisch, M.; Tetzlaff, A. Wind effect on PV module temperature: Analysis of different techniques for an accurate estimation. *Energy Procedia* **2013**, *40*, 77–86. [CrossRef]
43. Kaplani, E.; Kaplanis, S. Thermal modelling and experimental assessment of the dependence of PV module temperature on wind velocity and direction, module orientation and inclination. *Sol. Energy* **2014**, *107*, 443–460. [CrossRef]
44. Aelenei, L.; Pereira, R.; Gonçalves, H. BIPV/T versus BIPV/T-PCM: A numerical investigation of advanced system integrated into Solar XXI building façade. In Proceedings of the 2nd International Conference on Sustainable Energy Storage, Dublin, Ireland, 19–21 June 2013.
45. Kusuda, T.; Ta, T.A. Fundamentals of Building Heat Transfer. *J. Res. Natl. Bur. Stand.* **1977**, *82*, 97–106. [CrossRef]
46. Aelenei, L.E. *Thermal Performance of a Naturally Ventilated Cavity Wall*; Instituto Superior Técnico: Lisboa, Portugal, 2006.
47. Stine, W.B.; Harrigan, R.W. *Solar Energy Fundamentals and Design*; U.S. Department of Energy: Oak Ridge, TN, USA, 1985.
48. Tina, G.; Cosentino, F.; Notton, G. Effect of thermal gradient on electrical efficiency of hybrid PV/T. In Proceedings of the 25th European Photovoltaic Solar Energy Conference and Exhibition/5th World Conference on Photovoltaic Energy Conversion, Valencia, Spain, 6–10 September 2010; pp. 6–10.
49. Bot, K.; Aelenei, L.; Gonçalves, H. Design de um protótipo BIPVT e análise por meio de computação dinâmica de fluídos. In Proceedings of the CIES2020-XVII Congresso Ibérico e XIII Congresso Ibero-americano de Energia Solar, LNEG-Laboratório Nacional de Energia e Geologia, Lisbon, Portugal, 3–5 November 2020; pp. 1185–1192.